NOTICE

The quality of this microform is heavily dependent upon the quality of the original thesis submitted for microfilming. Every effort has been made to ensure the highest quality of reproduction possible.

If pages are missing, contact the university which granted the degree.

Some pages may have indistinct print especially if the original pages were typed with a poor typewriter ribbon or if the university sent us an inferior photocopy.

Reproduction in full or in part of this microform is governed by the Canadian Copyright Act, R.S.C. 1970, c. C-30, and subsequent amendments.

AVIS

La qualité de cette microforme dépend grandement de la qualité de la thèse soumise au microfilmage. Nous avons tout fait pour assurer une qualité supérieure de reproduction.

S'il manque des pages, veuillez communiquer avec l'université qui a conféré le grade.

La qualité d'impression de certaines pages peut laisser à désirer, surtout si les pages originales ont été dactylographiées à l'aide d'un ruban usé ou si l'université nous a fait parvenir une photocopie de qualité inférieure.

La reproduction, même partielle, de cette microforme est soumise à la Loi canadienne sur le droit d'auteur, SRC 1970, c. C-30, et ses amendements subséquents.

FEASIBILITY OF PRODUCING ^{186}Re, A POTENTIAL THERAPEUTIC RADIOISOTOPE

by

Suzanne P. Gardner
B.Sc., S.F.U., 1987

THESIS SUBMITTED IN PARTIAL FULFILLMENT OF THE REQUIREMENTS FOR THE DEGREE OF

MASTER OF SCIENCE

in the Department

of

Chemistry

SIMON FRASER UNIVERSITY

July, 1989

ISBN 0-315-59331-8

APPROVAL

Name: Suzanne P. Gardner

Degree: Master of Science (Chemistry)

Title of Thesis: Feasibility of Producing ^{186}Re, a Potential Therapeutic Radioisotope.

Examining Committee;

Chairman: P.W. Percival, Professor

Senior Supervisor: J.M. D'Auria, Professor

T.J. Ruth, TRIUMF

D. Sutton, Professor

Internal Examiner: R.J. Forteling, Professor

Date Approved: 9 Aug 1989

PARTIAL COPYRIGHT LICENSE

I hereby grant to Simon Fraser University the right to lend my thesis, project or extended essay (the title of which is shown below) to users of the Simon Fraser University Library, and to make partial or single copies only for such users or in response to a request from the library of any other university, or other educational institution, on its own behalf or for one of its users. I further agree that permission for multiple copying of this work for scholarly purposes may be granted by me or the Dean of Graduate Studies. It is understood that copying or publication of this work for financial gain shall not be allowed without my written permission.

Title of Thesis/Project/Extended Essay

Feasibility of Producing ^{186}Re, a Potential Therapeutic Radioisotope.

Author:

(signature)

Suzanne Gardner

(name)

10-08-89

(date)

ABSTRACT

^{186}Re is considered to be an attractive isotope for therapeutic applications due to its physical characteristics and its relationship to Tc. When coupled to monoclonal antibodies it is thought to be a powerful tool in the treatment of some forms of cancer. Current methods of production utilize the ^{185}Re(n,γ)^{186}Re reaction on enriched ^{185}Re. While this method has the advantage of a large reaction cross-section it does not achieve the high specific activities that are necessary for therapeutic use and often achievable using accelerator methods of production.

The feasibility of producing ^{186}Re using a new method of production which combines intermediate to high energy proton reactions with a simple, non-labour intensive chemical separation procedure has been investigated. This new method would be highly advantageous as it would provide a source of high specific activity, no carrier added ^{186}Re. To determine the feasibility of this approach two aspects of a production method were studied, rate of production using an accelerator, and a simple method of chemical separation.

First, the cross-section was measured for the production of ^{186}Re from foils of Au, Pt, and Ir. Thin foils were irradiated at TRIUMF with protons of energies from 200 to 500 MeV. The irradiated targets were analyzed using Ge(Li) gamma ray spectroscopy. The final cross-section for producing ^{186}Re proved to be significantly smaller than expected as

compared to calculations; upper limits were set. However due to the wealth of data available using gamma ray spectroscopy, cross-sections for Re, Ir, and Os spallation products were determined.

Second, a direct thermal separation method was investigated as a basis for developing a complete, simple, and fast method of separation. The release of Re, Ir, and Os isotopes from molten Au and Pt targets were studied using both a high temperature quartz tube furnace and a resistance heated, tantalum furnace system operated under vacuum. In both cases positive results were obtained indicating that this method could form the basis of a viable, fast separation scheme.

Acknowledgments:

I would like to thank Scott Tyldsely for his help with the irradiations, Mike Cackette for all his work on GXL, and Drs. John D'Auria and Tom Ruth for all their help.

TABLE OF CONTENTS

Approval	ii
Abstract	iii
Acknowledgments	v
Table of Contents	vi
List of Tables	viii
List of Figures	x
Introduction	1
^{186}Re as a Therapeutic Radioisotope	1
Cross-section of ^{186}Re	15
Separation Method	21
Experimental	29
Materials and Methods	29
Irradiations	29
Beam Integration	36
Data Acquisition and Analysis	39
Upper limit calculations - Method 1	44
Upper limit calculations - Method 2	45
Cross-section Calculations	46
Separation Procedure	47
Au target	48
Pt Target	52
Ir Target	56

Results and Discussion 57

^{186}Re Cross-section 57

Cross-sections of Ir, Os, Re, and Pt Isotopes 65

Au Target 73

Pt and Ir Targets 75

Separation Results 76

Au Target 76

Pt Target 80

Separation Discussion 84

Summary and Conclusions 86

Appendix A - SILT Calculations 88

Appendix B - Derivation of Beam Integration and Cross-section Equations 94

Appendix C - Sample Calculation of Cross-sections 98

References 102

LIST OF TABLES

1. Desired Physical and Chemical Characteristics 4

2. Physical Characteristics of ^{186}Re 9

3a. SILT Calculations - Au Target 17

3b. SILT Calculations - Pt and Ir Targets 18

4. Common Rhenium Oxides 24

5. Re Isotopes, Half Lives and Decay Modes 28

6. Target Thickness and Proton Energy 30

6. Beam Integtation Results 38

8. Cross-section for ^{186}Re, Ir Target 58

9. Cross-section Upper Limits for ^{186}Re, Au Target 58

10. Cross-section Upper Limits for ^{186}Re, Pt Target 58

11. Estimates of cyclotron time required to produce a single patient dose, 250 mCi, of ^{186}Re from Au, Pt, and Ir targets 62

12. Cross-sections of Ir, Os, Re, and Pt Isotopes, Au Target and Reference Values 67

13. Cross-sections of Ir, Os, Re, and Pt Isotopes, Pt and Ir Targets 68

14. List of Gamma Energies and Intensities used for Cross-section Calculations 69

15. Cross-sections as a Funtion of Gamma Energy and Proton Energy - Au target 70

16. Cross-sections as a Funtion of Gamma Energy and Proton Energy - Pt and Ir targets 71

17a. Separation Results - Au Target
Oven trial #1 77

17b. Separation Results - Au Target
Oven trial #2 78

18a. Separation Results - Pt Target
Evaporator trial #1 82

18b. Separation Results - Pt Target
Evaporator trial #2 83

A. Appendix A, Summary of Conditions for the use of Various Cross-section Equations 93

LIST OF FIGURES

1. Decay Scheme of ^{186}Re 8
2. ^{186}Re in relationship to other radioisotopes 16
3. Target Wheel 31
4. Sample Holder (Front view) 32
5. Target Package (Side view) 33
6. Beam line configuration 34
7. Dectector efficiency 40
8. Gamma Spectrum of Ir target 41
9. Gamma Spectrum of Ir target, energy region 110 - 200 keV 42
10. Quartz Insert for tube furnace 50
11. Quartz tube furnace set up in fumehood 51
12. Vacuum Evaporator Schematic 54
13. Vacuum Evaporator, Copper Electrodes 55
15. Distribution of released activity 79

A. Appendix A, Regions of applicability for various processes 92

INTRODUCTION

^{186}Re as a Therapeutic Radioisotope

^{186}Re, a beta emitting isotope, was first observed in 1935 by Soviet workers,[1] and later in 1939 by Sinma and Yamasaki[2]. Currently ^{186}Re is attracting interest within the nuclear medicine community for its potential use as a therapeutic radioisotope. The use of radiation in the diagnosis and treatment of some forms of cancer has focused on imaging techniques for diagnosis, such as ^{99m}Tc techniques, and external sources of radiation for therapeutic uses, conventional radiation therapy, and particle beam therapy using pions[3]. As these therapeutic methods are not site selective, they tend to result in high radiation doses to non-target areas. The ideal therapeutic method would deliver the maximum radiation dose to the target site with little or no radiation dose to surrounding organs and tissue. Labeling monoclonal antibodies with radioisotopes appears to be a step towards this ideal technique.

Labeling monoclonal antibodies with radioisotopes exploits the site specificity of the monoclonal antibodies[4,5,6,7,8,9]. Ideally an antibody can be grown that can be directed specifically towards cancerous cells. A labelled monoclonal antibody would then be capable of delivering a radiation dose directly to cancerous cells, lessening the radiation dose to other tissue. This methodology is currently used

for diagnostic purposes, especially with ^{99m}Tc, and is an active area of research for therapeutic applications.

To adapt this technique to therapeutic applications an appropriate radioisotope must be chosen. In selecting a radioisotope there are four basic questions that must be considered[10].

1) For what purpose is the labelled monoclonal antibody to be used? eg. diagnosis, therapy, follow-up, body burden evaluation, etc.

2) What are the desired physical characteristics of the radioisotope?

3) What chemical procedures will be used for incorporation of the radioisotope into the monoclonal antibody?

4) What is the expected radiation dose that will be delivered to the target area, and to the rest of the body and organs?

The final purpose of the labelled monoclonal antibody is an important factor as different purposes have different requirements. These differences are illustrated best by the desired physical characteristics. The main differences are in radiation dose; a diagnostic use requires minimal dose but a high abundance of imagable

radiation, while a therapeutic use requires a maximal dose but restricted to specific sites.

The question most pertinent to the choice of radioisotope is that of desired physical characteristics. By examining these characteristics one can determine which radioisotopes have potential. The characteristics vary depending on the end use of the labelled monoclonal antibody, and can be divided into two basic types, diagnostic and therapeutic. The desired physical and chemical properties for these two classes are presented in Table 1[10,11].

It is apparent that the two classes have some characteristics in common but also have other characteristics that are dramatically different. The half life of the isotope is important in ensuring that the radiation dose is delivered to the target site. The physical half life of the radioisotope must be compatible with the biological half lives both for the distribution and clearance of the monoclonal antibody. If the physical half life of the radioisotope is too short it is possible that the majority of the isotope will have decayed prior to the monoclonal antibody accumulating in the target areas. Alternatively if the half life of the isotope is too long the monoclonal antibodies may start clearing from the body before a significant portion of the radioisotope has decayed.

TABLE 1

DESIRED PHYSICAL AND CHEMICAL CHARACTERISTICS[10,11]

PROPERTY	COMMENTS: DIAGNOSTIC USE	COMMENTS: THERAPEUTIC USE
Radionuclide half life	Short, compatible with biological distributions (6h - 8d)	Short, allow localzation at cancerous sites, (6 - 200 h)
Gamma energies & intensities	High intensity, (80 - 240 keV)	Low intensity to minimize dose to non-target areas
Photon yield per absorbed radiation dose	High abundance, single energy, per dose	Small abundance per dose
Parent-daughter relationship	Stable decay products	Stable decay products
Ratio penetrating to non-penetrating radiation	Enough penetrating to allow imaging, little non-penetrating	Higher non-penetrating than penetrating, to maximize dose to target.
Particle radiation	None, or low abundance, low energy	High abundance particulate radiation, high LET
Production mode	Availability	Availability
Stability of radionuclide-protein bond	Required to transport radionuclide to desired site	Same
Specific activity	High as possible	Same
Retention of immunological nature as function of amount of carrier	Antibody should not change in nature with radioactive label.	Same
Nonradioactive carrier	Minimize	Same

The parent-daughter relationship is the same for both cases. The daughter should be stable to radioactive decay, preventing secondary radiation doses[12].

Gamma energies and intensities are characteristics which vary depending on use. A diagnostic use requires an isotope with a high intensity or abundance of gammas of an energy that can be imaged. Preferably a single energy gamma per decay. A therapeutic use on the other hand requires a low abundance or intensity of gammas to minimize the dose to non-target tissue, although a low intensity gamma of imagable energy is desirable in order to image the distribution of the radiation throughout the body. For diagnostic radioisotopes a high intensity of gammas is desired to obtain imaging with the smallest possible dose of radiation. For therapeutic radioisotopes a low intensity is desired as much higher doses of radiation are used.

To accompany a diagnostic isotope there should be little or no non-penetrating radiation, minimizing overall dose. Conversely a therapeutic isotope must have a high ratio of non-penetrating to penetrating radiation as it is the non-penetrating radiation which provides the therapeutic dose.

A therapeutic isotope should have a high abundance of medium to high LET (linear energy transfer) particulate radiation, either alpha, (high LET), or beta, (medium LET). The choice of alpha or beta radiation depends on the type of cancer to be treated. Alpha particles

deposit large amounts of their energy over very short ranges, beta particles have lower LET values but have a slightly longer range. Alpha particles may be better for very small target areas or areas that can be uniformly permeated with the monoclonal antibody while beta particles may be more suited for larger target areas or areas that the monoclonal antibody cannot penetrate uniformly.

Whether they be diagnostic or therapeutic, the production mode of the radioisotopes determines the availability. A production method is desired that can provide a high specific activity source of the radioisotope in a useful chemical form. The production method must consider the actual production of the isotope using nuclear reactions and the chemistry that is required to separate and isolate it.

Finally, in both cases it is very important that the monoclonal antibody radioisotope bond be stable, and that the labeling of the antibody does not affect its biological function.

There are many isotopes which satisfy the physical criteria, including: ^{67}Cu, ^{186}Re, ^{188}Re, ^{90}Y, ^{109}Pd, ^{131}I, ^{123}I, ^{212}Bi, ^{197}Hg, ^{32}P[11]. Of these ^{186}Re seems to be one of the more promising as it satisfies the desired criteria[8,13,14], and has the added advantage that it belongs to the same periodic group as ^{99m}Tc, a diagnostic radioisotope, for which there exists a large body of chemical data applicable to Re. ^{188}Re is also a potential therapeutic radioisotope. ^{186}Re is preferred over ^{188}Re due to the half life, and gamma

energy.[9] The decay scheme[1] of ^{186}Re, Figure 1, and the Table of Physical Characteristics (Table 2) outline the relevant characteristics of ^{186}Re. With a half life of 90.6 hours, the predominant decay route is beta emission (E_{max} = 1.07 MeV) to ^{186}Os, excited states of which decay via emission of gamma and x-rays, the most abundant one a 137.2 keV gamma, with an intensity of 9.2%. ^{186}Os is essentially stable, it decays via alpha emission but with an extremely long half life, $\approx 2 * 10^{15}$ years. The secondary decay route is via electron capture to the stable ^{186}W isotope. The half life of ^{188}Re is shorter at 16.98 hours, and has a more intense gamma of higher energy, 155.0 keV at 14.9 %.[1] The gamma emission of ^{186}Re is closer to that of ^{99m}Tc, 140.5 keV, meaning that gamma cameras used for ^{99m}Tc could also be used for ^{186}Re. Most gamma cameras are specifically designed for use with ^{99m}Tc.[13]

Figure 1 - Decay scheme of ^{186}Re.[1]

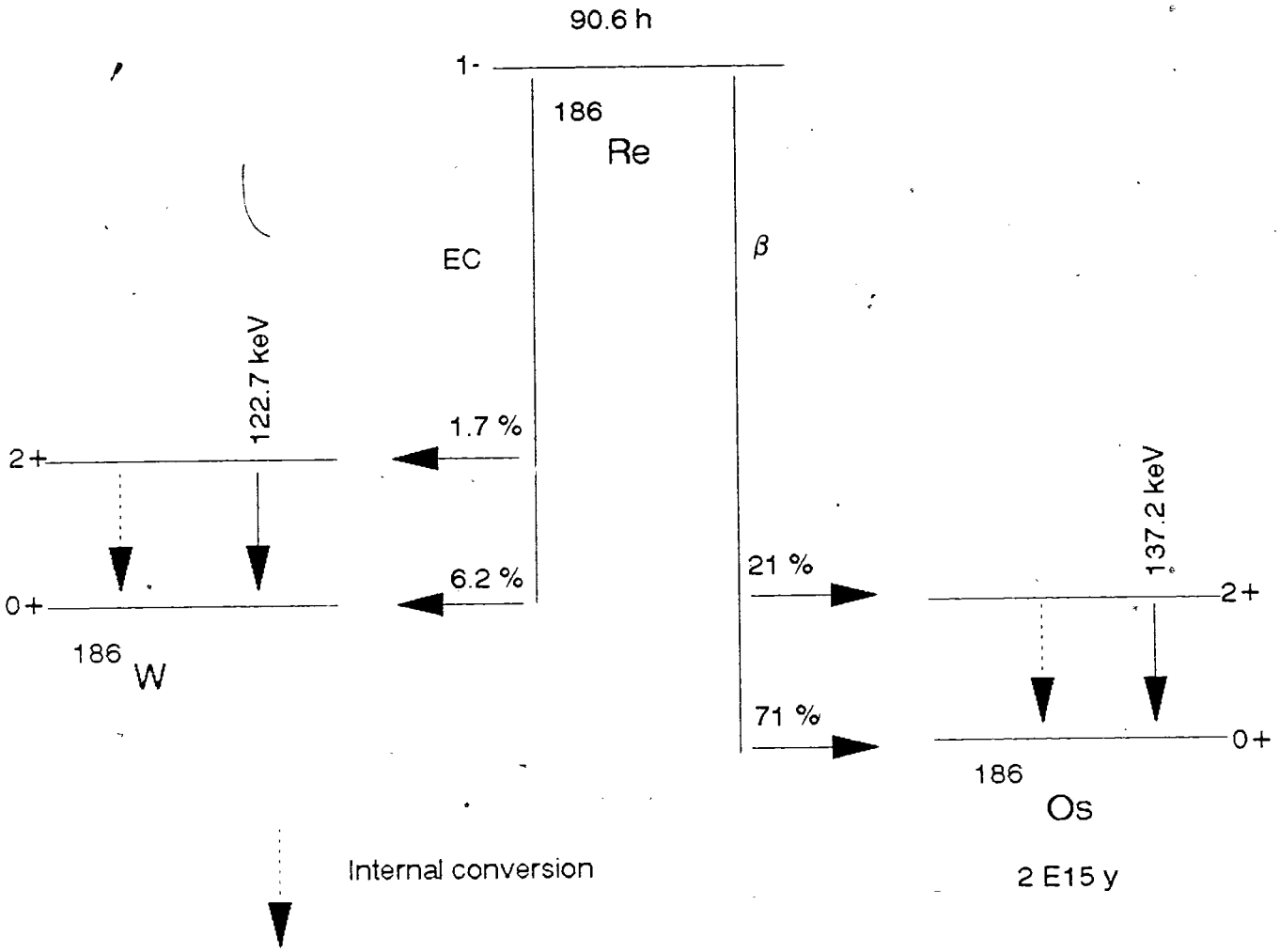

TABLE 2

PHYSICAL CHARACTERISTICS OF ^{186}Re

$T_{1/2}$	90.6 h	
Decay	92.2 % beta 7.8 % EC	E_{max} = 1.070 MeV
E_γ	137.2 keV (9.2%) 122.7 keV (0.72%)	
Daughters	^{186}Os ($t_{1/2}$ $2*10^{15}$ y) ^{186}W (stable)	
Max. Specific Activity	$1.28 * 10^3$ GBq/μmol	

The fact that Re is in the same periodic group as Tc is an advanage since they should exhibit similar chemical properties and techniques developed for ^{99m}Tc should be ammenable to use with ^{186}Re.[8,14,15] In comparing the three members of the group, Mn, Tc, and Re, Tc and Re are more similar to each other than either is to Mn. This is due to the "lanthanide contraction", the filling of the 4f orbitals which are ineffective in shielding the 5d electrons from the nucleus. The 5d electrons experience a relatively large effective nuclear charge, which causes rhenium to be much smaller than expected. In the free metals Re and Tc have virtually identical atomic radii, and in many complexes the Re and Tc crystal radii will be very similar. Therefore the properties which depend on physical size and charge such as, size, shape, dipole moment, formal charge, ionic mobility, and lipophilicity should be the same or similar for analogous Tc and Re complexes. Rhenium and technetium are similar chemically in that they both form stable oxides in high oxidation states, the heptoxides being the most common. Both heptoxides are water soluble and form hydrogen pertechnetate ($HTcO_4$) and perrhenic ($HReO_4$) acids.

As mentioned previously, ^{99m}Tc has been used extensively for diagnostic purposes. Recently advances have been made in labeling monoclonal antibodies with $^{99m}Tc^{6}$, in which the form of technetium used for the labeling is hydrogen pertechnetate. This should also be feasible with the rhenium analogue.

While some chemical properties may be similar, there are

differences which may affect the behavior of Re complexes compared to analogous Tc complexes. Re is more stable in higher oxidation states, making it more difficult to reduce than Tc[16]. This is problematic since if Re is present in the radiopharmaceutical in a reduced form it may easily be oxidized back to perrhenate, destroying the radiopharmaceutical. Another difference is in the size of ligand field splitting: as Re has a larger ligand field splitting, ligand substitution onto the metal centre will be slower than for Tc. This could affect the time frames for some chemical syntheses. This problem could probably be easily overcome by testing the Tc synthesis with stable rhenium.

Procedures for conjugating Tc and Re to monoclonal antibodies have been developed recently[6]. One common procedure is to use bifunctional chelating agents to conjugate the metal to the antibody. This type of conjugation is favoured as the conjugation of the metal to the antibody does not interfere with any of the functional groups on the antibody. Direct labelling is not used as it is very difficult to find a site on the antibody that could be exchanged with a metal atom. It is very important that the addition of a metal atom does not change the behavior of the monoclonal antibody *in vivo*.

The mechanisms for using ^{186}Re conjugated to monoclonal antibodies are in place, and preliminary work[8,9,16,17] is underway on rats. The major drawback to using ^{186}Re is the availability. Currently ^{186}Re is produced via the neutron capture reaction of enriched ^{185}Re,

$^{185}Re(n,\gamma)^{186}Re$. Although cross-sections for neutron capture reactions are generally large, ≈100 mb[8], this production route is not favored as it is difficult to achieve high specific activities. Specific activity being defined as the number of nuclei decaying per unit time per unit mass of material present[18]. It is possible to calculate the maximum possible specific activity for any radioisotope using Equation 1

$$\text{SpAct (Bq/g)} = \frac{C}{t_{\frac{1}{2}} * A} \qquad C = 4.174 * 10^{23} \qquad (1)$$

$t_{\frac{1}{2}}$ = half life in seconds

A = atomic weight

The constant C incorporates Avogadro's number to convert from moles to number of atoms, and *ln*2 to convert the half life into a decay constant. This equation is based on determining the number of radioactive atoms present in one gram of pure ^{186}Re. The resulting maximum possible specific activity for ^{186}Re is $1.28 * 10^6$ GBq/mmol[19]. The specific activity of ^{186}Re produced via the neutron reaction was only 50 Ci/mmol or $1.85 * 10^3$ GBq/mmol[8]. Typical neutron irradiations are 24 hours in length using neutron fluxes of $\approx 10^{14}$ n/s-cm^2, on 86% enriched ^{185}Re.[8,16]

Accelerator based reactions, *i.e.* charged particle reactions, tend to produce higher specific activity products, because the target material is in general a different element. Trials were performed by Nordion International investigating the reaction of low energy protons, < 20 MeV, on ^{186}W, $^{186}W(p,n)^{186}Re$. The results indicated a maximum

yield of 50 μCi/μA-hr[20]. This yield is too low to be economically feasible for therapeutic uses. At a typical patient dose of $\geq$ 250 mCi, at least thirty hours of cyclotron time would be required[21].

The approach taken in this work was to investigate the possibility of using spallation of high Z targets with high energy protons[22]. This method was thought to be viable because although spallation reaction cross-sections tend to be low, on the order of 10 mb[22], high yields should be attainable due to the target thickness that can be used. When working with high energy protons thick targets can be used without appreciable energy degradation resulting in higher yields than can be obtained by methods that must use thin targets. The major drawback to this approach is the very large number of products formed in spallation reactions including all the other Re isotopes along with ^{186}Re. Hence a method is needed to separate the ^{186}Re from the soup of products; not a trivial process. There is a relatively simple separation method available for the separation of rhenium from molten gold. This method utilizes the volatility of rhenium oxides which are formed at high temperatures and allow rhenium to be released from molten metals.[15] This method was investigated and is discussed later.

Au was chosen as the main target for this work because of the existence of a separation technique. Pt was chosen as it was thought that it should exhibit behavior similar to Au as they are both noble metals. Ir was chosen due to its proximity to Re, and it should have a higher cross-section. Other less expensive targets, such as Pb and Hg;

were not considered for the following reasons. Pb as a target, is well known to have very specific release properties. The only element released from Pb is Hg.[23] The thermal method of separation investigated in this work would not be applicable to Pb. Hg was not considered as a target as it is a liquid with a very high vapour pressure, which may cause separation problems. It is difficult to handle and is known to be toxic.[24] Another potential target, Os, was not investigated. Although it is likely to have a larger cross-section for production of ^{186}Re than Ir, it is not available as a foil, making it difficult to work with, and is very expensive.

This work involved determining the feasibility of producing ^{186}Re from proton spallation reactions of Au, Pt, and Ir, and separating rhenium from the metal targets.

CROSS-SECTION OF ^{186}Re

An extensive literature search revealed no published values for the cross-section of ^{186}Re produced from high energy proton reactions on any of the selected targets.

As can be seen from Figure 2, ^{186}Re is a shielded isotope, that is there are no radioactive isotopes which decay to ^{186}Re. This makes ^{186}Re of interest to the nuclear chemist because it can provide a clean test of reaction theories, since it is not produced by the decay of any other radioisotopes. In general the overall production yield for shielded isotopes is much smaller than for non-shielded isotopes, and requires direct measurement. The difference in production yields for shielded and non-shielded isotopes exists due to the summing up of cross-sections that occurs for non-shielded isotopes. Before the cross-section determination was attempted the cross-section was estimated using calculations based on the Silberberg and Tsao method[25,26]. The Silberberg and Tsao method is discussed in more detail in Appendix A. These calculations are summarized in table 3, and indicate that the cross-section should be on the order of 1-15 mb.

Figure 2

^{186}Re in relationship to other radioisotopes

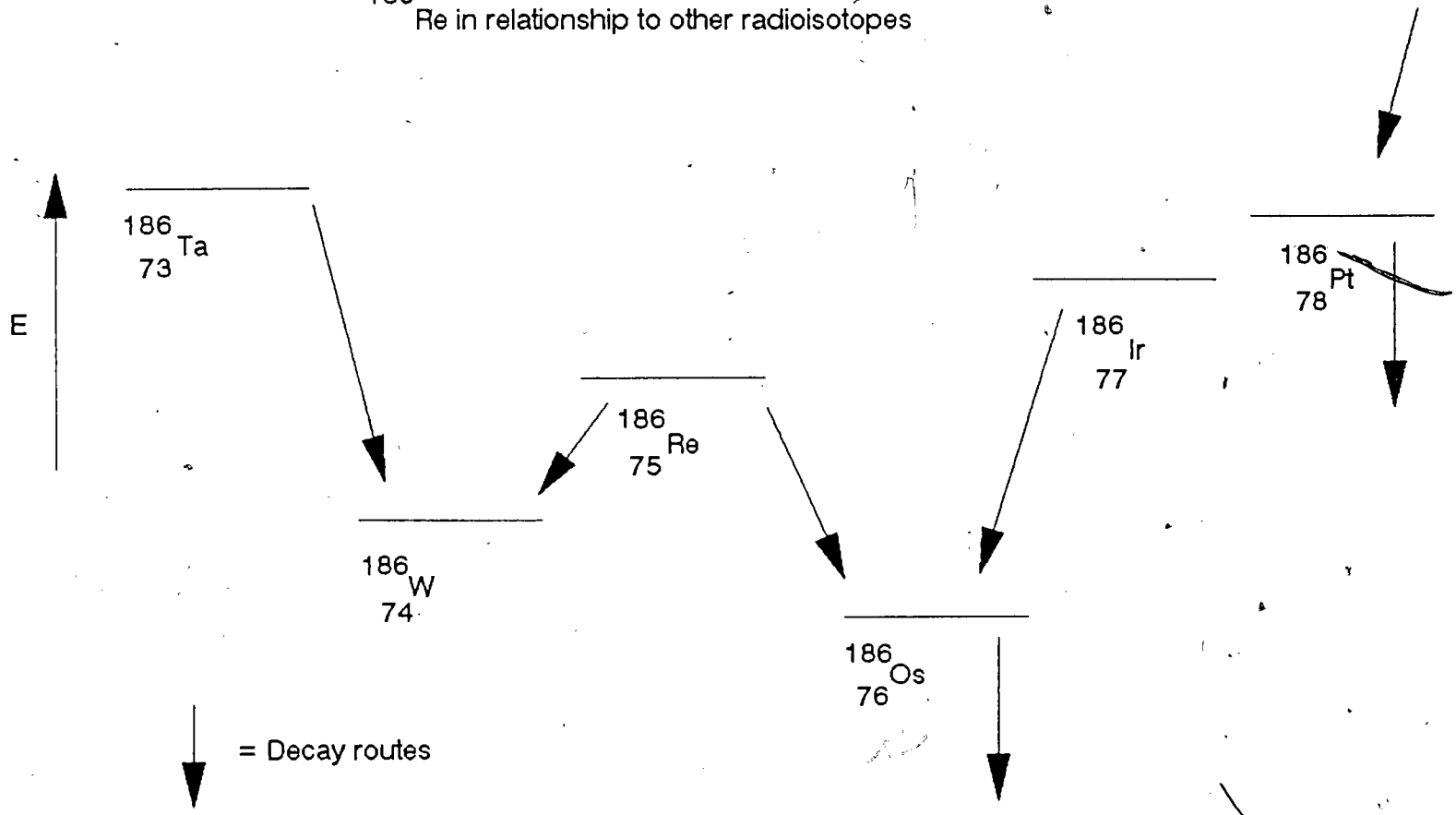

TABLE 3a

SILT CALCULATIONS

Au TARGET

Isotope	Cross-section (mb) at Energy (MeV)				
	200	300	400	500	600
^{186}Ir	29.8	41.7	56.6	66.8	61.8
^{189}Ir	10.5	9.82	9.23	8.76	8.39
^{190}Ir	6.95	6.17	5.5	4.97	4.57
^{192}Ir	0.66	0.70	0.74	0.75	0.75
^{194}Ir	0.17	0.21	0.25	0.26	0.26
^{182}Os	13.0	25.7	42.1	56.1	58.1
^{183}Os	12.1	22.0	34.3	44.5	44.8
^{185}Os	9.83	15.0	21.4	26.0	24.7
^{191}Os	0.64	0.58	0.62	0.63	0.62
^{181}Re	5.09	11.0	18.9	25.9	27.7
^{182}Re	3.67	7.27	11.9	15.9	16.5
^{183}Re	3.29	5.98	9.34	12.1	12.1
^{184}Re	1.95	3.25	4.84	6.07	5.94
^{186}Re	0.76	1.07	1.41	1.71	1.58
^{188}Pt	20.8	20.9	21.1	21.3	23.5

TABLE 3b

SILT CALCULATIONS

Pt TARGET

Isotope	Cross-section (mb) at Energy (MeV)					Isotope	
	200	300	400	500	600		500
^{186}Ir	88.3	98.4	111.7	121.3	118.1	^{186}Ir	103.4
^{189}Ir	155.0	138.22	124.03	112.7	103.9	^{189}Ir	142.5
^{190}Ir	172.7	151.77	133.8	119.7	108.5	^{190}Ir	143.9
^{192}Ir	193.0	167.3	144.1	127.4	113.9	^{192}Ir	66.5
^{194}Ir	111.7	102.7	94.45	87.3	81.6	^{194}Ir	——
^{182}Os	75.93	126.7	189.9	239.2	235.8	^{182}Os	40.8
^{183}Os	82.55	128.5	185.6	228.3	220.2	^{183}Os	44.7
^{185}Os	68.6	87.8	111.4	129.1	125.2	^{185}Os	55.5
^{191}Os	7.95	7.36	6.82	6.32	5.92	^{191}Os	31.4
^{181}Re	38.96	73.5	119.2	155.6	160.1	^{181}Re	86.5
^{182}Re	30.52	53.5	82.4	105.7	106.1	^{182}Re	57.6
^{183}Re	29.2	47.3	69.9	87.2	85.5	^{183}Re	32.5
^{184}Re	18.35	27.4	38.84	47.23	44.96	^{184}Re	20.05
^{186}Re	7.97	10.15	13.15	15.12	14.72	^{186}Re	6.02
^{188}Pt	233.3	214.4	199.2	187.4	177.6	^{188}Pt	——

Ir TARGET

^{186}Re is observed through the detection of a 137.2 keV gamma ray from the decay of ^{186}Os[1]. Unfortunately, ^{186}Ir also decays to ^{186}Os and exhibits the same characteristic 137.2 keV gamma. This leads to problems in distinguishing the two isotopes. The half life of ^{186}Ir is 15.8 hours, a factor of $\approx$ 6 smaller than that of ^{186}Re. This difference is large enough that if ^{186}Ir and ^{186}Re were present in equal initial activities it is possible to separate the two isotopes as two components of a half life plot. If however there is a large excess of ^{186}Ir it becomes difficult if not impossible to distinguish how much of the activity is due to ^{186}Re.

There are many radioisotopes which decay with more than one gamma ray. This provides an internal check of results, as the radioisotope can be identified by more than one gamma energy. ^{186}Re only has one gamma in reasonable intensity, its other gammas are either of too low energy to be detected or of too low intensity.[27] ^{186}Ir has numerous other gammas which are of sufficient intensity and energy to be used as verification of the 137.2 keV gamma. In analysis these other gammas can be used to help determine how much of the activity is due to ^{186}Ir and how much is due to ^{186}Re. The 434.8 keV gamma of ^{186}Ir is especially useful as it arises solely from ^{186}Ir, making analysis simpler.[27]

Spallation reactions produce many different products. The most abundant products of a spallation reaction are those within 10 - 20 mass units of the target on the low mass side. Abundant products tend to be towards the neutron deficient side of beta stability. As many of these

products will be unstable and will involve the emission of one or more gammas in their decay, a gamma spectrum of a target following spallation will be very complicated due to the large numbers of observed peaks. This excess of information can make identifying isotopes difficult, but it can also be very useful. Cross-sections can be determined for products for which spallation cross-sections are known and can be used for confirming results. There are at least two published papers[28,29] on cross-sections of spallation products of gold targets. A third set of results would be useful to confirm previous results to clarify any differences which may currently be present.

SEPARATION METHOD

In order for a radioisotope to be of use medically it must be available in a pure, sterile, and pyrogen free state[30]. The sterility and pyrogen free aspects usually arise in the final form of the radioisotope, eg. incorporated in a biological molecule. The purity takes on two forms, that of the purity of the molecule the radioisotope is attached to, and the specific activity of the radioisotope. In order to be usable a specific activity of ≈4 Ci/mg is required, this defines the amount of carrier that is allowed and therefore the purity of the radioisotope.[31] When faced with the myriad of products of a spallation reaction, arriving at this specific activty of radioisotope is difficult.

There are numerous methods used for separating and isolating radioactive products[32,33]. Four common techniques are; distillation, precipitation, solvent extraction, and ion exchange. Distillation techniques involve the volatilization of the species to be separated which is collected either by cooling or absorption on an appropriate substance. This method is highly dependent on the volatility of the species to be separated and on the characteristics of the target material. Precipitation is a fairly common technique and is often used in conjunction with one or more of the other techniques. The techniques are often adapted from classical analytical techniques and often require dissolution of the target material and the availability of a selective

precipitation reagent or reagents. Solvent extraction offers high selectivity and high yields can be obtained by successive extractions and back extractions. Again the target material must be dissolved and the technique can be difficult to adapt to remote operation. Remote procedures are almost essential with the high levels of radioactivity that are present when radioisotopes are being produced for medical purposes. Ion exchange methods are extensively used, and the wide range of ion exchangers available makes them very selective techniques, capable of high yields. The majority of these techniques involve dissolution of the target and separation from a solution. This type of separation can be difficult, depending on the ease with which the target can be dissolved. Dissolving the target is also a disadvantage if the target material is very expensive. The targets used in this work, Au, Pt, and Ir, are all fairly expensive and difficult to dissolve. Au and Pt both require aqua regia for dissolution, while the recommended solvent for Ir is concentrated HCl + $NaClO_3$ at 125 - 150°C[15]. The ideal separation technique would allow for easy recovery of the target so it could be used repeatedly. For these reasons the distillation technique is clearly the most advantageous. A variation of this technique is discussed here for the separation of metallic isotopes, as their oxides from target materials.

A method used for separating one metallic species from a metallic target is thermochromatography. Thermochromatography is, as the name suggests, a chromatographic technique that utilizes condensation temperature as the characteristic by which elements or compounds can be

separated. The element or compound to be separated must be volatilized, then released down a column with a negative temperature gradient, the volatile species will condense out along the column according to their condensation temperatures. It is apparent that this method will only be applicable to elements or compounds which can easily be volatilized. The main element of interest in this work, rhenium, has a very high melting point (3180°C)[24], and a boiling point of over 5500°C[24] rendering it next to impossible to volatilize directly. However previous work has shown that rhenium can quite successfully be separated using this technique since in the presence of oxygen, even in trace amounts, volatile rhenium oxides are formed. The five stable rhenium oxides are listed in Table 4.

Table 4

Common Rhenium Oxides

$Re_2O_3 \cdot xH_2O$
ReO_2
ReO_3
Re_2O_5
Re_2O_7

Of these five, the heptaoxide, Re_2O_7, is the most stable. The lower oxides all decompose to the heptaoxide at temperatures above ≈300°C [15]. The heptaoxide is also known to be volatile at temperatures above ≈500°C [15].

Previous thermochromatographic work[34-39] showed that rhenium could be separated from gold targets in high efficiencies, and that the separation was free from impurities of other volatile oxides, such as iridium or osmium oxides which condense at much lower temperatures. The experimental procedure used was to melt an irradiated gold target which had been fused to the end of a quartz tube, then to pass a flow of He or other gas over the melt into the thermochromatographic column. The column was then cut into pieces and analyzed with gamma spectroscopy in order to determine what isotopes condensed out at what temperatures.[35] As it was apparent that rhenium could be released from molten gold it seems likely that a similar process could occur with platinum. Both gold and platinum are noble metals and would be expected to behave similarly. The major difference is that platinum, with a melting point of 1772°C[24], is somewhat more difficult to melt. Most laboratory furnaces reach a maximum temperature of 1200°C. This method of separation is advantageous as it allows for recovery of the target material, and lends itself to further development with on- or off-line mass spectroscopy, which can provide the necessary isotopic separation.

One disadvantage of all of the above mentioned techniques is that while they are element selective they are not isotope selective. It is very important, in the production of radiopharmaceuticals, to have reasonable isotopic purity. If one looks at the possible Re isotopes that may be formed in a spallation reaction, Table 5[40] , one can see that there is a wide range of half lives, and decay modes possible. Contamination with any of these other isotopes may cause the effects of the labelled molecule to deviate from what is desired and reduce the specific activity of ^{186}Re. One method of separating isotopes is to use mass spectroscopy, a widely used technique. The use of an ISOL (Isotope Separation On-Line) facility is also possible for on-line production and separation. ISOL facilities use mass spectroscopy techniques in the final mass separation component. ISOL systems have three major components: ion production, ion beam transport, and isotope collection[23,41]. Ion production encompasses the production and ionization of the ions. Ion beam transport encompasses transporting the ion beam to a mass spectrometer, and transporting the outgoing mass separated ion beams. Finally isotope collection encompasses collection and detection of the separated isotopes. If spallation reactions are ever to become a source of radioisotopes for medical purposes, a mass spectroscopy type separator, or possibly an ISOL system will probably become a necessity. It is possible that a target system could be designed that used a molten metal target, the products would volatilize out of the molten metal, be collected on a cold finger of appropriate temperature, to allow for chemical separation, and then volatilized into an ion source, and finally separated by mass. The resolution for

separation on ISOL systems is very high, on the order of 10,000 : 1 separation[23]. If successful, these types of techniques could produce many different isotopes of the same element simultaneously.

TABLE 5

Re Isotopes, Half Lives and Decay Modes

Isotope	Half Life	Decay Mode
^{170}Re	8 s	EC
^{172}Re	30 s	EC
^{174}Re	2.2 m	EC
^{175}Re	5 m	EC
^{176}Re	5.7 m	EC
^{177}Re	14 m	EC
^{178}Re	13.2 m	EC, β^+
^{179}Re	20 m	EC, β^+
^{180}Re	2.45 m	EC, β^+
^{181}Re	19 h	EC
^{182}Re	12.7 h	EC, β^+
^{182m}Re	64 h	EC
^{183}Re	70 d	EC
^{184}Re	165 d	EC, IT
^{184m}Re	38 d	EC
^{186}Re	90.6 h	β^-
^{188}Re	17 h	β^-
^{189}Re	24 h	β^-
^{190}Re	3 h	β^-
^{191}Re	9.7 m	β^-
^{192}Re	16 s	β^-

EXPERIMENTAL

Materials and Methods

Irradiations

Thin foils of Au, Pt, and Ir were irradiated at the TRIUMF cyclotron facility (Vancouver, B.C.) with protons of energies ranging from 235 to 500 MeV. Specifications of the targets and the irradiations are compiled in Table 6.

All target materials were obtained from Johnson Matthey Chemicals Ltd. and had the following compositions: Au-99.998%, Pt-99.998%, and Ir-99.9%.

A target holder system was designed, by the author, and built, by the S.F.U. mechanical shop, to allow for irradiation of the targets in air on beam line 4A at TRIUMF. A portion of the beam pipe was removed in order to accommodate the target wheel, Figure 3. The target wheel was aligned with the centre of the beam pipe, and could be operated remotely. The targets were cut into 2.5 * 2.5 cm squares, packaged into sample holders, and placed in the target wheel. Sample holders, target packages, and the beam-line configuration are illustrated in Figures 4, 5, and 6.

Table 6

Target Thickness and Proton Energy

Target	Thickness mg/cm^2	Proton Energy MeV
Au1	198.648	500
Au2	198.648	290
Au3	198.648	370
Au4	198.648	235
Au5	198.648	445
Au6	198.648	500
Pt1	217.044	290
Pt2	217.044	500
Pt3	217.044	235
Pt4	217.044	370
Ir1	102.512	500

Figure 3

TARGET WHEEL

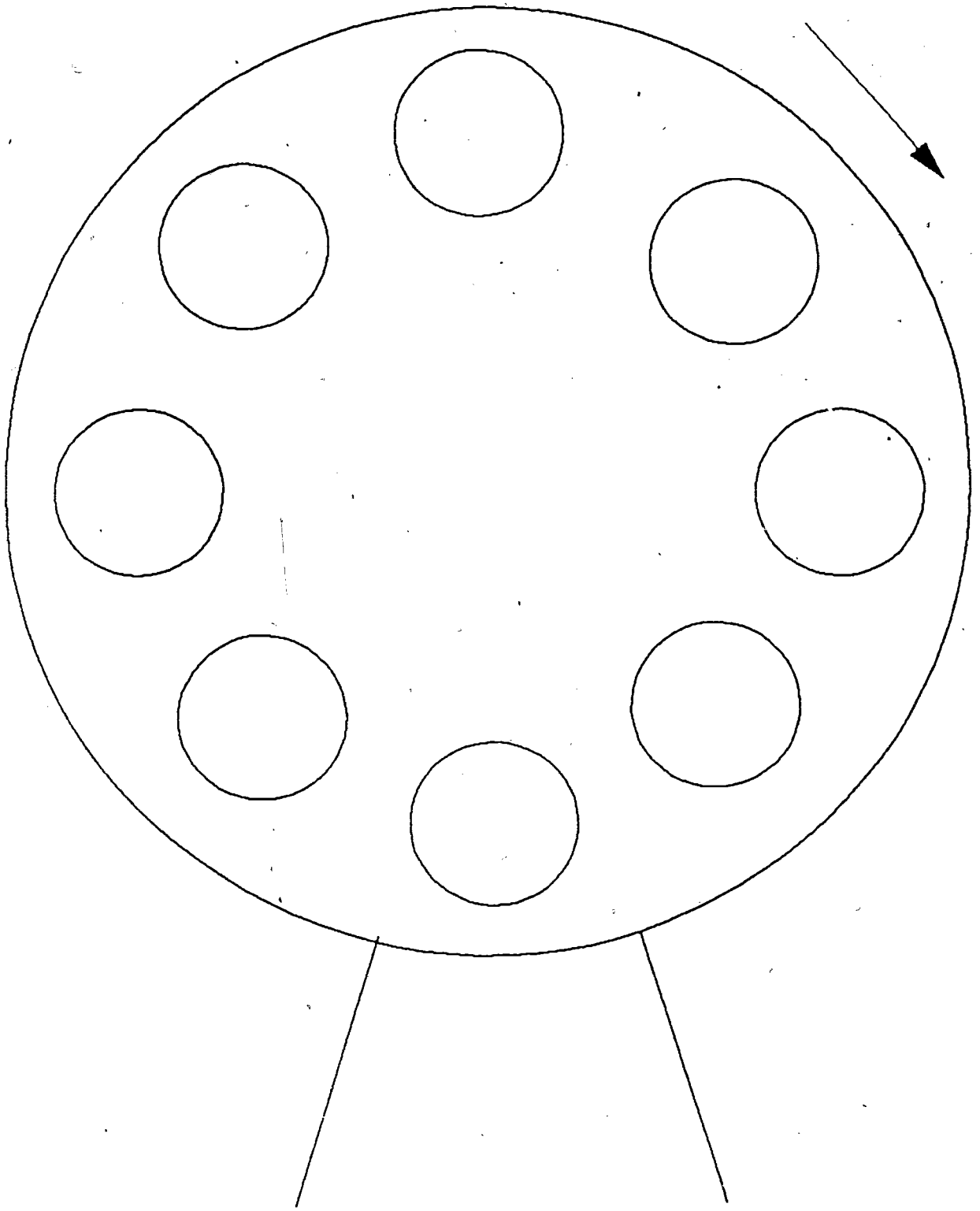

Figure 4 Sample Holder (Front view)

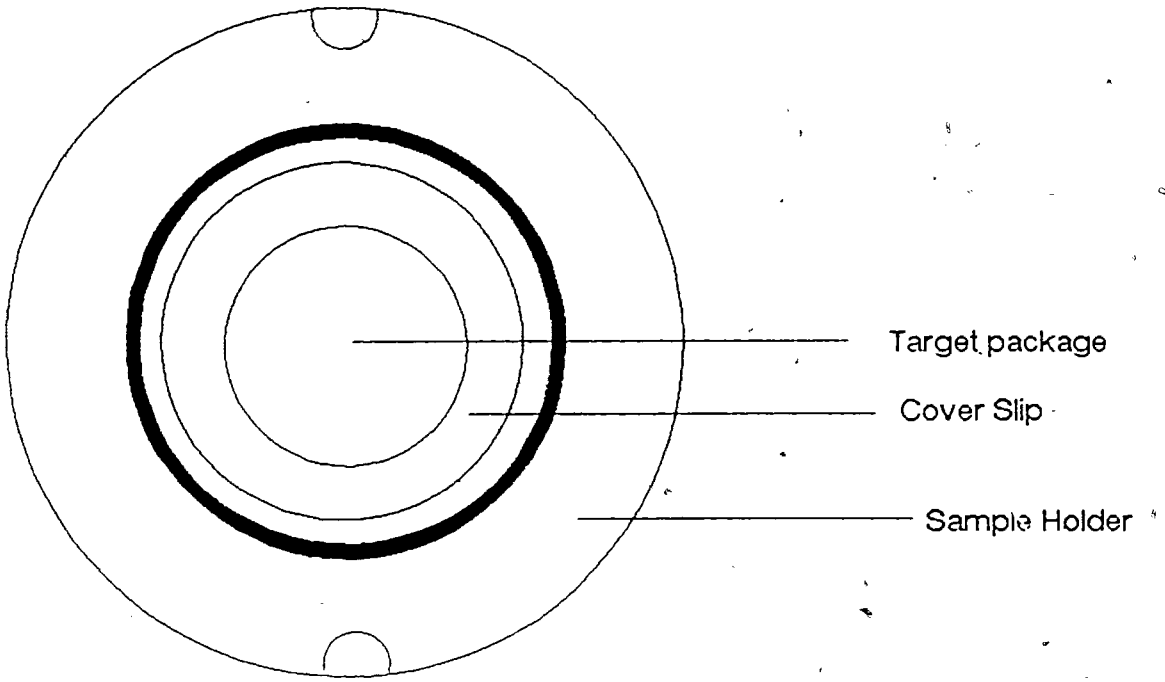

Figure 5 Target Package (Side view)

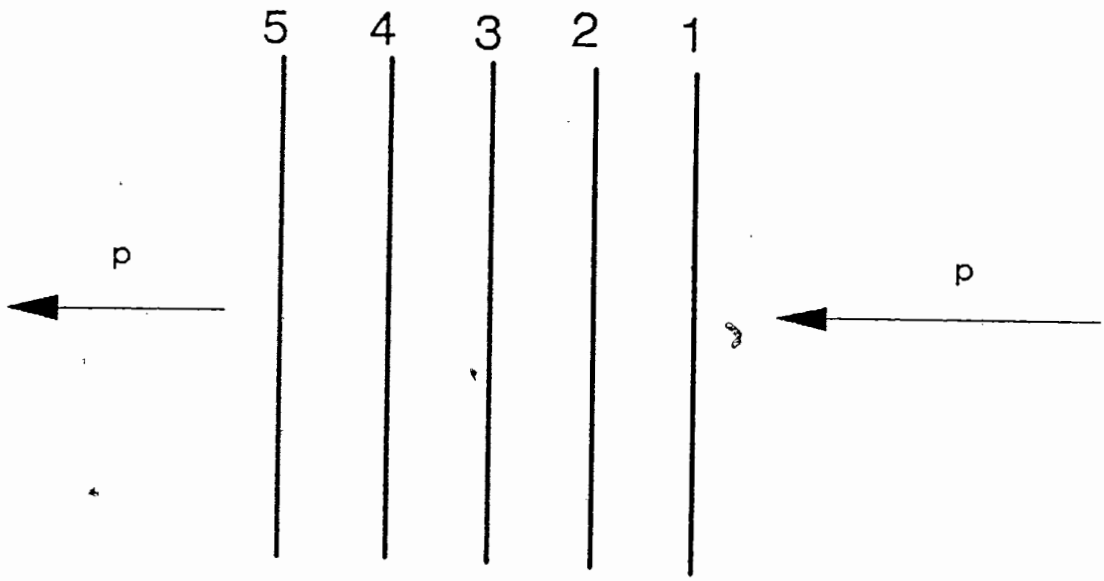

1 = Al foil 0.007mm

2 = Al foil 0.007mm

3 = Al foil 0.007mm

4 = Metal foil (Au, Pt, Ir)

5 = Al foil 0.007mm

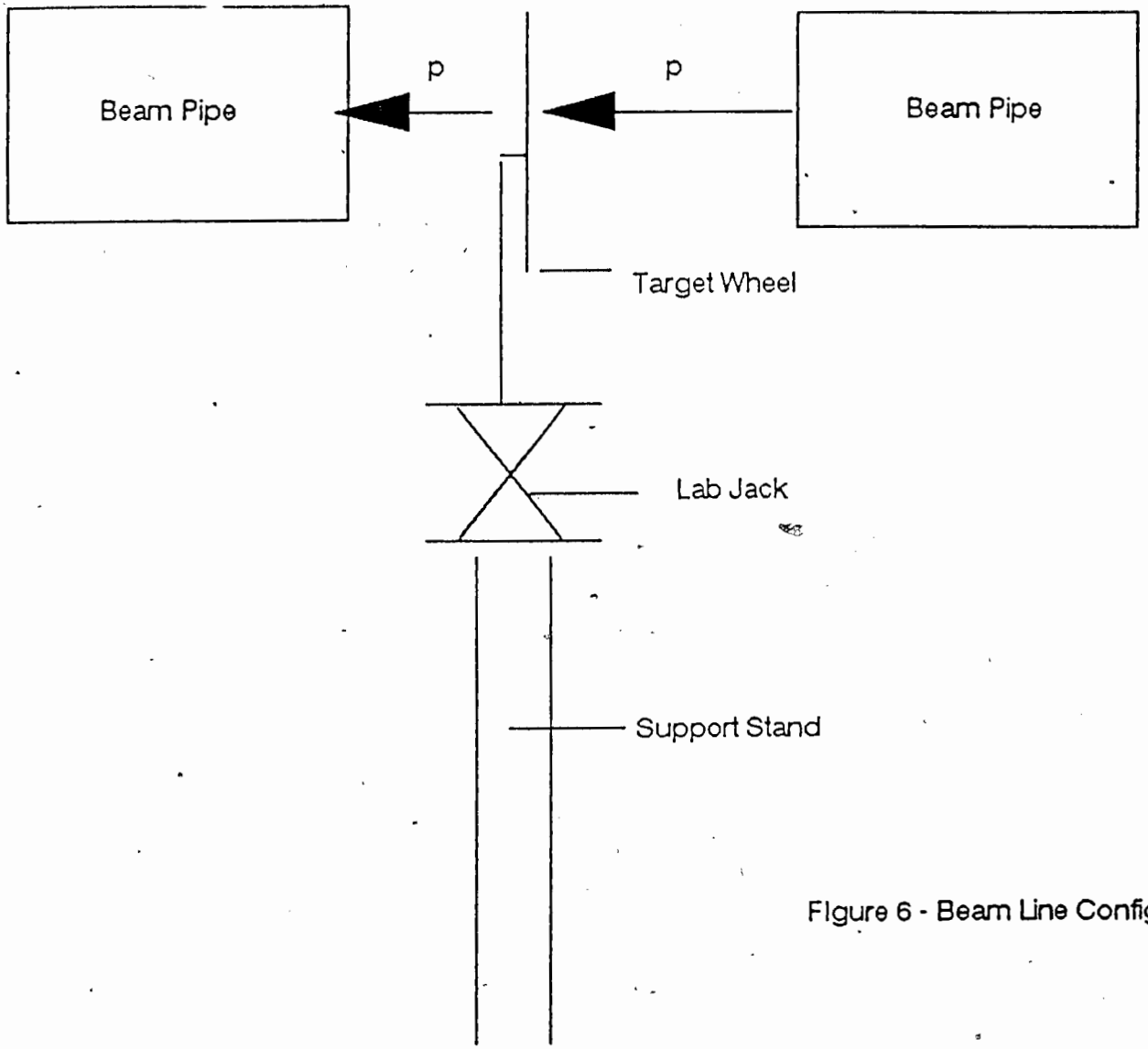

Figure 6 - Beam Line Configuration

Alignment of the proton beam and target wheel was checked by short (three minute) irradiations of lucite targets. The targets were inspected visually to ensure the beam was properly aligned, with the sample holders. A darkening of the lucite indicated the alignment of the proton beam.

All proton irradiations were at beam currents of either ≈0.5 μA or ≈1.0 μA, and for periods ranging from 20 minutes to one hour.

Due to the high radioactivity of the targets after irradiation, the target packages were allowed to cool before being removed from the sample holders and transported to S.F.U., where they were analysed using gamma ray spectroscopy.

Beam Integration

During irradiations the instantaneous beam flux was monitored with the in-beam SEM (secondary electron emission monitor) to determine the time uniformity of the irradiation. The beam size was < 1 cm in diameter, smaller than the target area. The actual total beam current, incident on the target, was calculated by measuring ^{24}Na production in thin Al monitor foils. ^{24}Na is produced by the $^{27}Al(p,3pn)^{24}Na$ reaction. The cross-section for this reaction is known, to ±6.5%, for energies from 30 MeV to 30 GeV, and is a commonly used monitor reaction[42]. Al foil #2, Figure 5, was used as the monitor foil to as any ^{24}Na lost through recoil would be replaced by ^{24}Na recoiling from the front foil.

The Al monitor foils from each target package were counted using a standard Ge(Li) gamma-ray spectroscopy detector system. The 1368.53 keV gamma of ^{24}Na ($t_{½}$ = 15.03 h)[1] was detected and areas for this gamma peak were determined manually on a Nuclear Data ND66 multi-channel analyser.

The total number of protons for each irradiation was determined using Equation 2:

$$\Phi = \frac{A_{EOB}}{\epsilon * \lambda * N(t) * \sigma} \qquad (2)$$

Where;

A_{EOB} = activity at end of bombardment (cps)

ϵ = detector efficiency

λ = decay constant for ^{24}Na

N(t) = Al target thickness (atoms/cm^2)

σ = cross-section for ^{24}Na

The derivation of Equation 2 and equations to follow is detailed in Appendix B. The largest error proved to be the 6.5% error on the literature values of σ. Other contributing errors are the errors in measuring peak areas and therfore in determining A_{EOB}, and in the detector efficiency. A summary of the calculations and the relative errors are presented in Table 7. These values agreed with the approximate values obtained with the in-beam SEM.

Table 7

Beam Integration Results

Target	Φ (p)
Au1	1.63E+16 ± 8.9 %
Au2	1.22E+16 ± 8.9 %
Au3	3.83E+15 ± 7.8 %
Au4	3.39E+15 ± 8.4 %
Au5	3.71E+15 ± 7.8 %
Au6	4.03E+15 ± 8.4 %
Pt1	1.41E+16 ± 8.9 %
Pt2	1.59E+16 ± 8.9 %
Pt3	3.44E+15 ± 8.4 %
Pt4	1.19E+16 ± 7.6 %
Ir1	3.88E+15 ± 8.4 %

Data Acquisition and Analysis

Gamma spectra of all foils were collected using a standard Ge(Li) gamma-ray spectroscopy detection system, including standard nucleonics, coupled to a Nuclear Data ND66 multi-channel analyser. The detection system was calibrated using standard ^{133}Ba and ^{137}Cs sources, whose gamma energies include some similar to those of ^{186}Re. Total detector efficiencies were determined for all geometries used, by plotting logarithmic plots of efficiency versus energy for the standard sources. An example of an efficiency curve is illustrated in Figure 8. The spectra were analysed and peaks fit by using either of the spectra fitting programs GXL[43] on the IBMPC or GAMANAL[44] on the MTS mainframe. The peaks were analysed using either of the half life fitting programs CLSQ[45] on the TRIUMF VAX or FRANTIC[46] on the IBMPC.

A number of problems were encountered throughout the data acquisition and analysis. Initially spectra were collected over 1024 channels, for an energy range of 0 - 1 MeV. This range was insufficient for the number of peaks in the spectra and made fitting the spectra difficult if not impossible. The channel range was subsequently increased to 2048 channels. Typical gamma spectra are illustrated in Figures 8 and 9. As can easily be seen there are a very large number of peaks. In some cases, there were not enough fitted spectra collected to perform half life analysis. This was the case for the foils from the first irradiation for which 1024 channel spectra had been collected that could not be fit. These targets did have enough data to calculate upper limit cross-sections.

POWER	0	1
COEFFICIENTS	-.18949	-.86542
STD DEVNS	.19131	3.22199E-02

WEIGHTED STD DEVN OF FIT =5.076E-02

X	Y EXP	Y CALC	DEVN
5.079	-4.6574	-4.5849	7.246E-02
5.622	-5.0030	-5.0549	-5.187E-02
5.713	-5.0973	-5.1336	-3.632E-02
5.875	-5.2404	-5.2738	-3.342E-02
5.950	-5.3143	-5.3387	-2.442E-02
6.236	-5.6107	-5.5862	2.447E-02
6.495	-5.8174	-5.8104	7.024E-03
7.150	-6.4279	-6.3772	5.068E-02

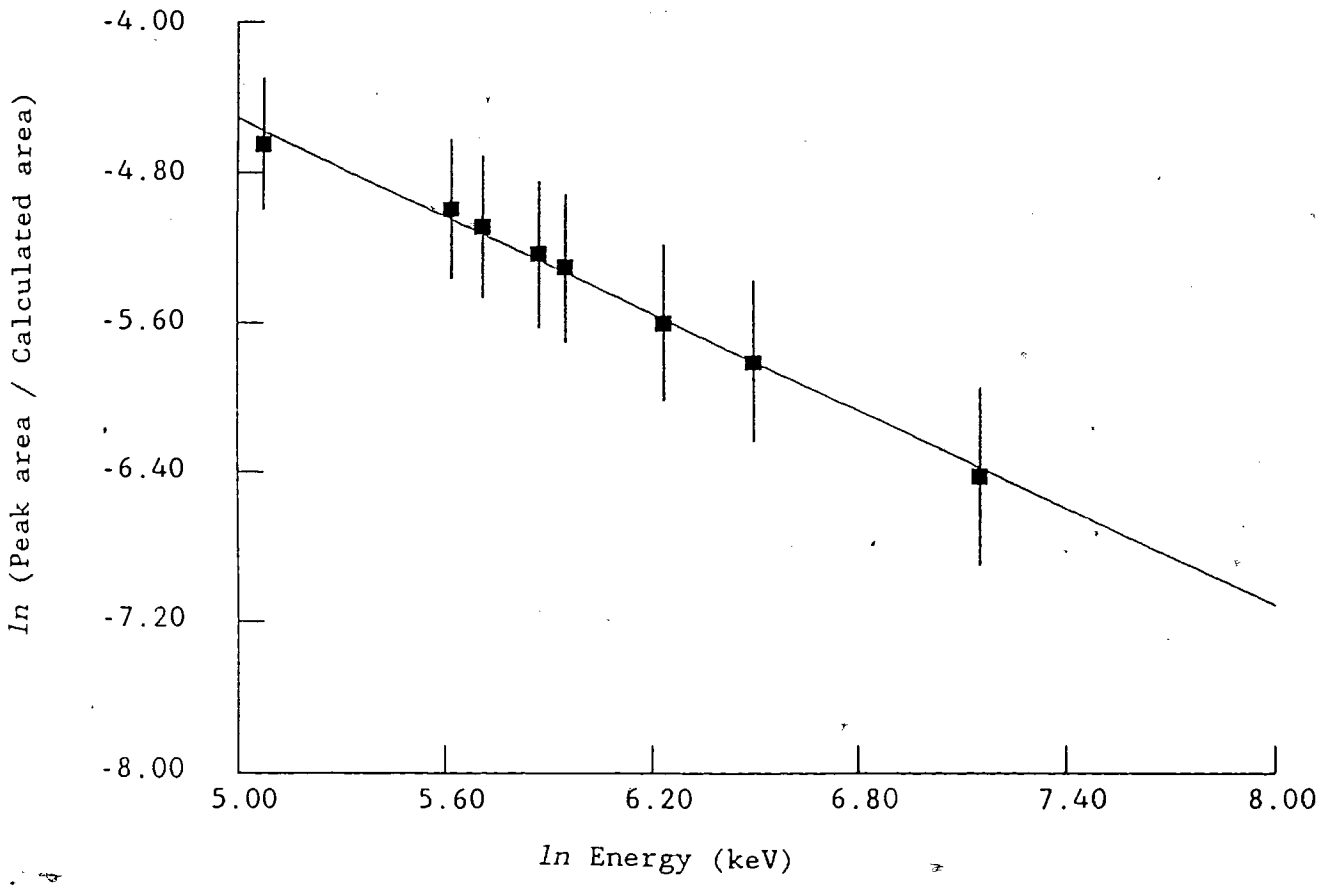

Figure 8 - Detector efficiency.
Detector gain = 20.5
Position = 7

Figure 8 - Gamma Spectra of Ir target.

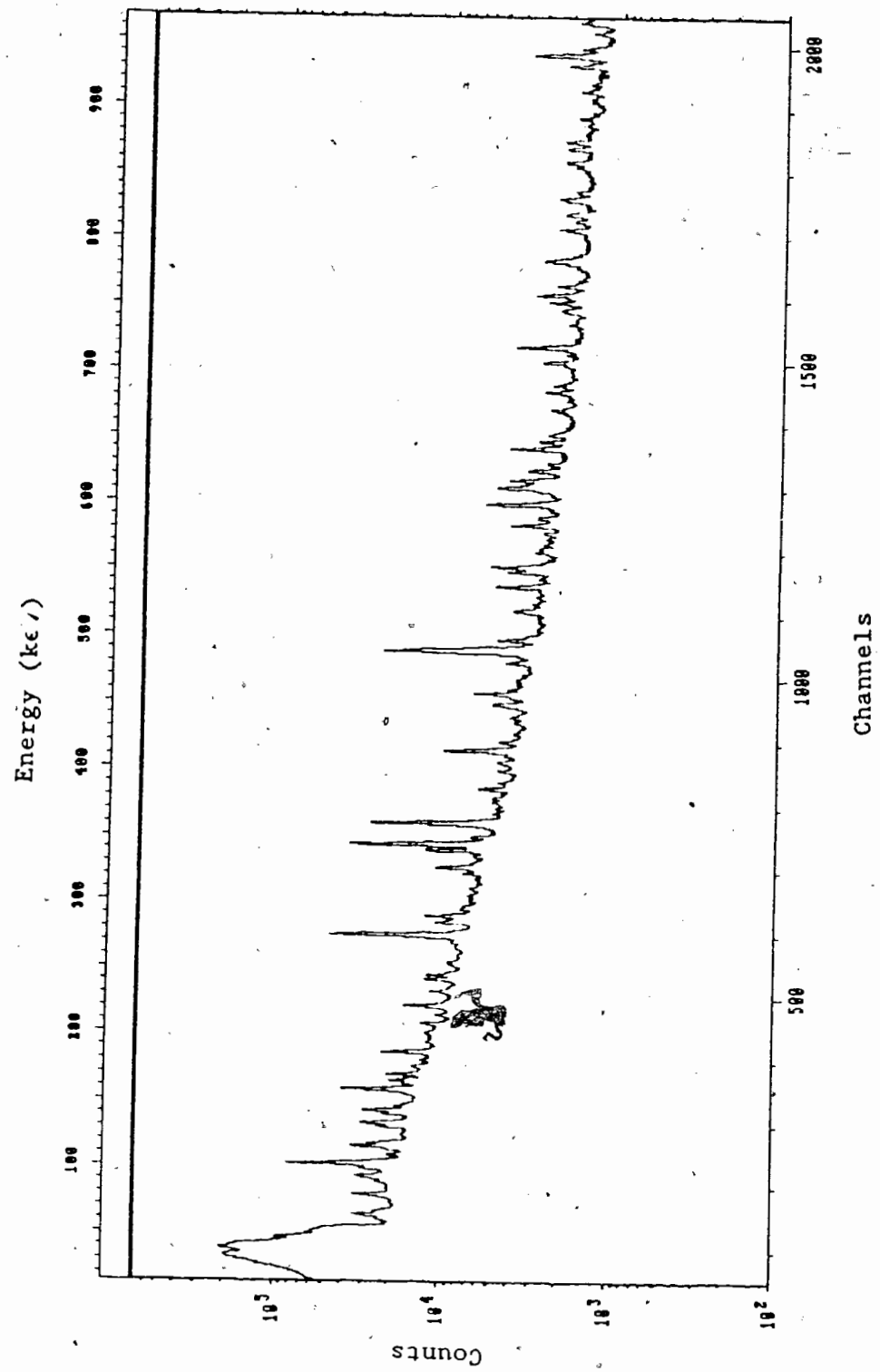

Figure 9 - Gamma spectrum of Ir target, energy region 110 - 200 keV.

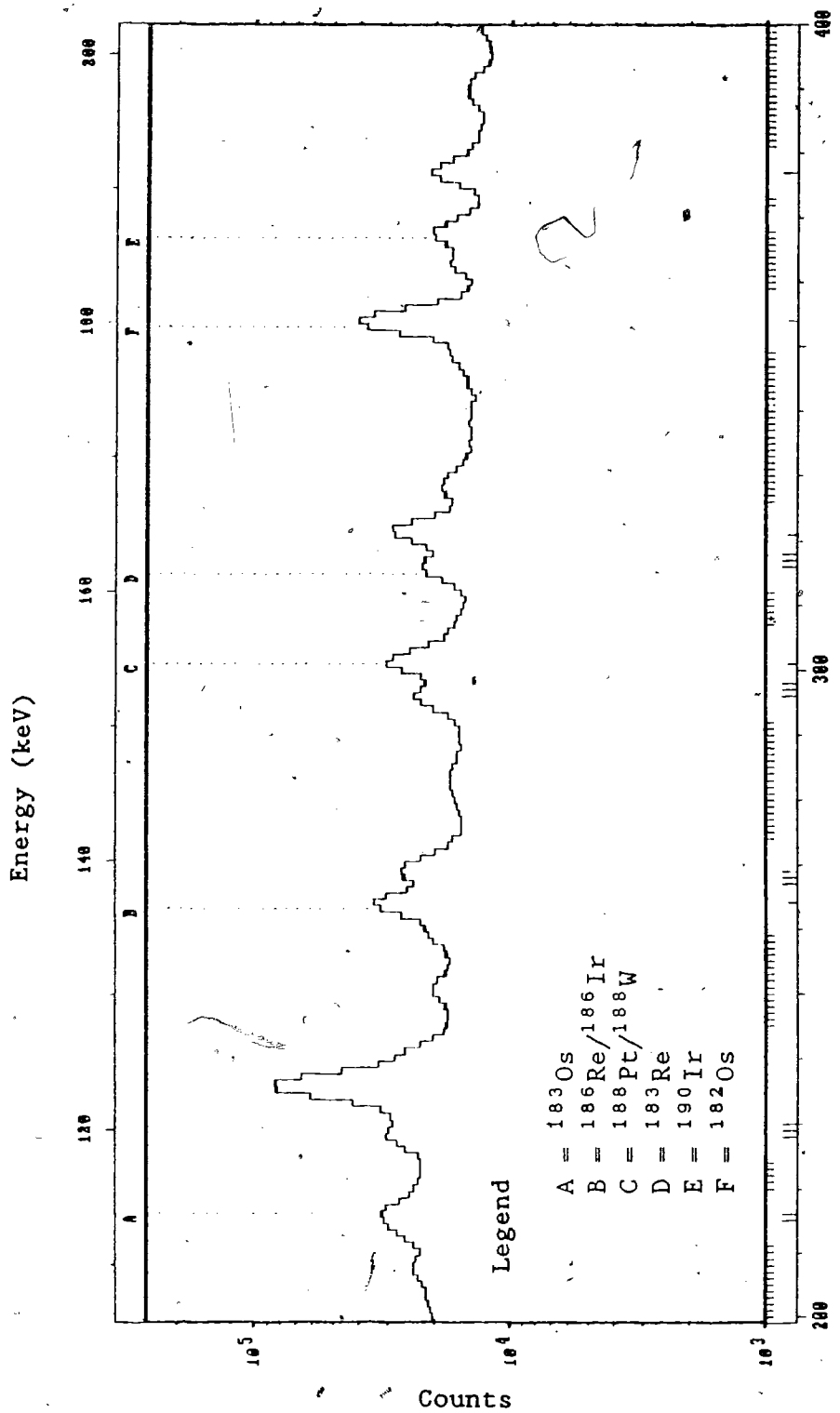

Although the main goal of this work was to calculate the cross-section for ^{186}Re, in all but one case this was impossible. ^{186}Ir also emits gamma radiation of 137.2 keV and although the ratio of the half lives of ^{186}Re and ^{186}Ir appears to be sufficient that the individual components should be distinguishable, the amount of ^{186}Ir produced far exceeds the amount of ^{186}Re produced completely obscuring the ^{186}Re. Only in one case, that of the Ir target, was it possible to fit the two components to the experimental data. In all other cases upper-limits on the ^{186}Re cross-section were set.

The results from the half life fitting programs for other gamma peaks were used to calculate cross-sections for other spallation products.

Upper-limit calculations - Method 1

Using a spectrum collected after a sufficiently long time, approximately 10 days after irradiation, so that the majority if not all of the ^{186}Ir had decayed, upper limits on the ^{186}Re cross-section were determined using the following method.

The maximum possible peak area that could be present, but not observable above background, was determined to be three times the square root of the background over the region where the 137.2 keV gamma should appear[47]. This value was corrected to EOB (end of bombardment) and upper limits calculated using Equation 3:

$$U.L.\sigma_{^{186}Re} = \frac{A_{EOB}}{N(t) * \Phi * \epsilon * b * \lambda} \qquad (3)$$

where;

$U.L.\sigma_{^{186}Re}$ = upper limit cross-section

A_{EOB} = activity corrected to end of bombardment (cps)

$N(t)$ = target thickness (atoms/cm^2)

Φ = total number of protons as calculated from ^{24}Na production

ϵ = detector efficiency for appropriate energy and geometry

λ = decay constant

b = branching ratio for gamma radiation

Upper-limit calculations - Method 2

The time at which the 137.2 keV peak could no longer be observed was determined.

The number of ^{186}Ir and ^{186}Re half lives that had elapsed over this time were calculated.

The maximum possible amount of ^{186}Re that could be present at end of bombardment was calculated to be the ^{186}Ir A_{EOB} divided by 2 to the power x, where x is the difference between the number of ^{186}Ir half lives and ^{186}Re half lives elapsed.

Equation 3 was used with the maximum A_{EOB} for ^{186}Re to determine cross-section upper limits.

Cross-section

Results from half life fitting programs were used to calculate experimental cross-sections. The results given by the half life fitting programs had previously been corrected for detector efficiency and corrected back to EOB. Equation 4 was used for calculating the cross-sections:

$$\sigma = \frac{A_{EOB}}{N(t) * \Phi * b * \lambda} \qquad (4)$$

where;

A_{EOB} = activity at EOB, efficiency corrected (cps)

$N(t)$ = target thickness (atoms/cm^2)

Φ = total number of protons as calculated from ^{24}Na production

b = branching ratio for gamma radiation

λ = decay constant

In order to illustrate the analysis procedure, one case, that of ^{186}Re and ^{186}Ir, 137.2 keV gamma, Ir target, has been detailed in Appendix C.

Other results were obtained in a similar manner. When possible more than one gamma peak was used and the cross-section reported as the average ± associated error. See Tables 12 and 13 for results.

SEPARATION PROCEDURE

The basis for a fast, simple separation technique was investigated for the Au and Pt target foils. It is very important that the technique be simple in nature and, due to the high levels of radioactivity, involve minimal hands-on contact. The basis of the technique is the release of volatile oxides of rhenium from molten metals. The goals of the experiments were to melt the targets and measure the release of Re isotopes from the molten targets. The main difficulty encountered was in finding methods to melt the target materials.

The procedures used for each target are discussed, results are discussed later.

Au Target

A quartz tube furnace was constructed using Thermcraft® heating elements and a specially designed quartz insert. The heating elements were powered by a 220V power supply and regulated with a 220V variac. The heating elements were rated to 1200°C, more than adequate for melting the Au target (Au m.p. 1063°C)[24]. The quartz insert was designed with inlet tubes for a thermocouple, and gas, outlet tube for gas, and detachable sample holders or "spoons". The quartz insert and sample "spoons" are pictured in Figure 10. A chromel-alumel thermocouple was used for measuring temperature, and a calibrated flow meter was used for controlling gas flow. The outlet tube was air cooled and connected to a U-trap cooled to 0°C. The complete experimental set up is illustrated in Figure 11.

After testing the furnace and calibrating the variac, two experimental runs were completed. A gamma spectrum of the sample, (¼ of one of the Au targets) was initially collected. The sample was placed in the sample "spoon" and the furnace assembled. The temperature was brought up to ≈1100°C and allowed to equilibrate. Medical quality air was then passed through the quartz insert at a rate of ≈20ml/min for a period of 20 minutes. At this point the power to the furnace was turned off and the furnace was allowed to cool overnight. The following day the furnace was disassembled and gamma spectra of all components collected. The spectra were analysed using the GAMANAL[44] program. By

comparing the activities present in the target before and after heating, it was possible to determine which radioisotopes were released and in what percentages. The gamma spectra of the furnace components indicated where the released activity was deposited. A second run was completed using the same procedure with the exception of a static atmosphere instead of air flow. Results were calculated for each case by determining percent released for the visible radioisotopes. As these experiments were completed long after the target irradiations, long lived radioisotopes such as ^{183}Re and ^{185}Os were used as the primary indicators, making the assumption that all isomers of a specific Z value will behave identically.

Figure 10 - Quartz insert for tube furnace.

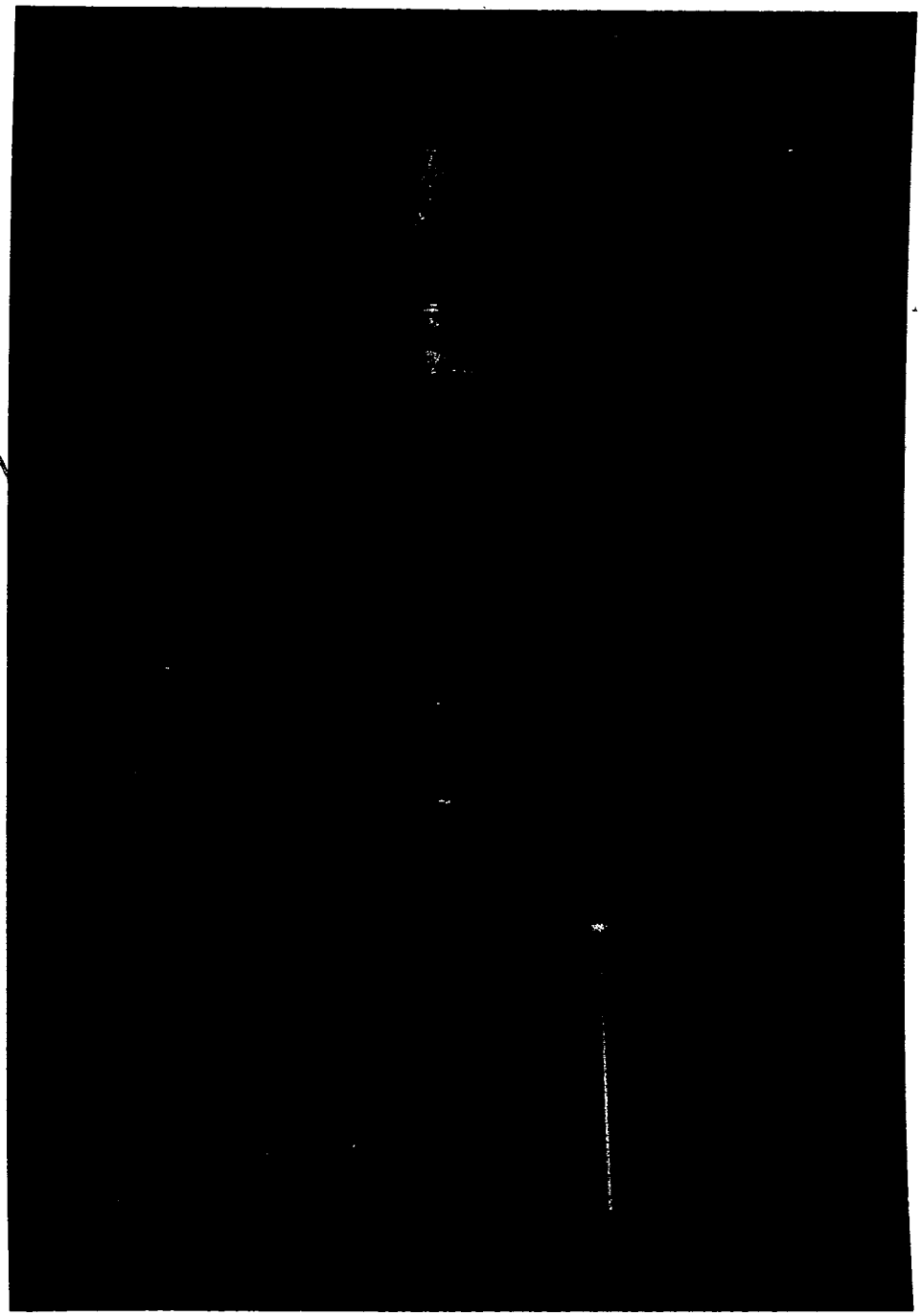

Figure 11 - Quartz tube furnace set up in fumehood.

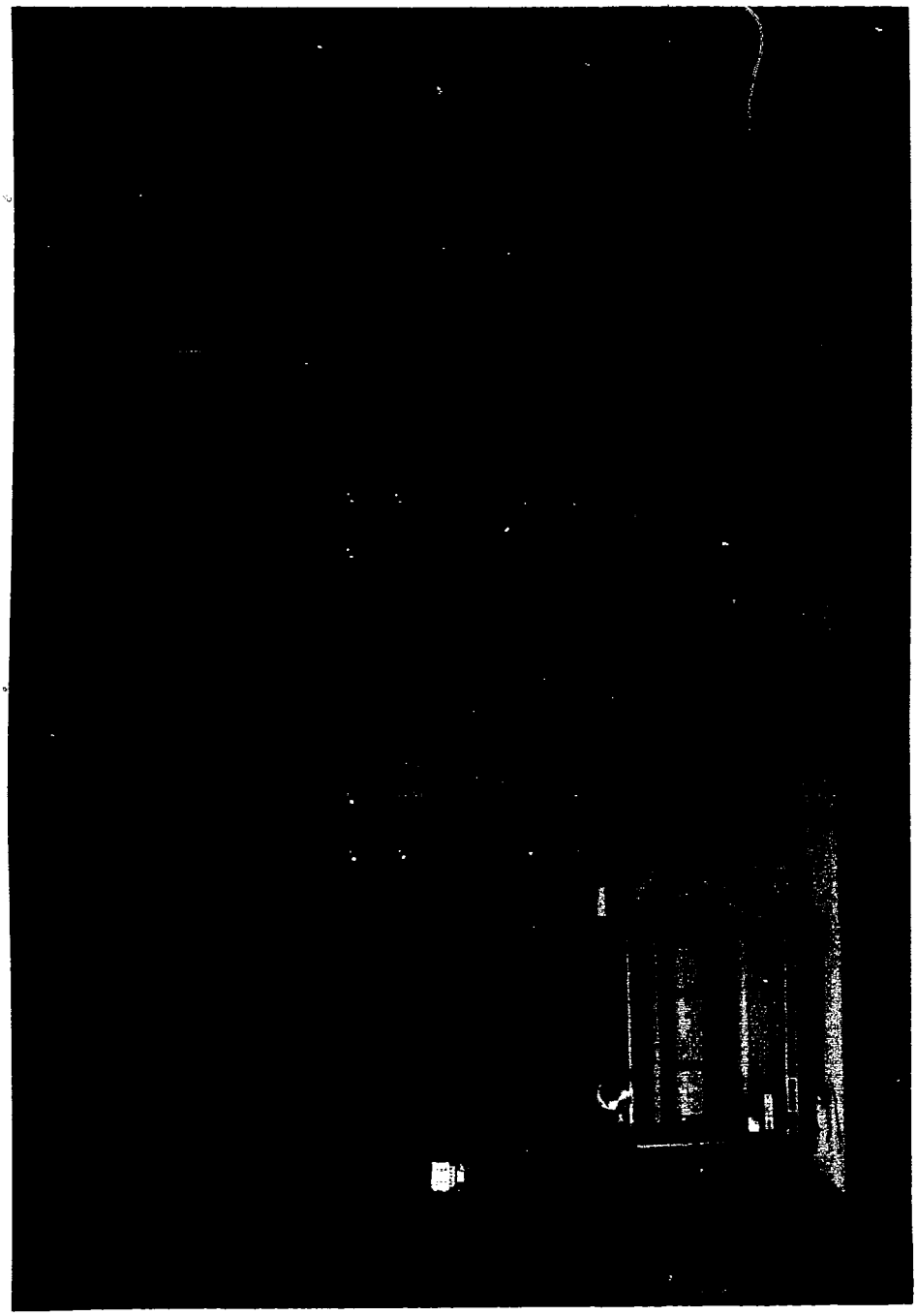

Pt Target

As the tube furnace was only capable of reaching 1200°C a different method was required to melt the Pt target, (m.p. 1772°C)[24]. A resistance heated tantulum furnace system operated under vacuum, (vacuum evaporator), Figure 12[48], located at TRIUMF was used. Under optimal conditions this system is capable of reaching ≈2000°C. Heating is achieved by passing electrical current through a metal sample holder clamped between two copper electrodes, Figure 13[48]. The maximum attainable temperature is very dependent on the shape, thickness, and material used for the sample holder. A variety of Ta sample holders were tested, varying thickness of the foil and shape of the sample holder. The configuration giving the highest temperature was that of a BN (boron nitride) crucible wrapped in 0.5mm Ta foil. This resulted in an external temperature of ≈1700°C ± 100°C as measured by using a pyrometer. There is error in the temperature measurement due to the difficulty in using a pyrometer, and the inability to determine if the temperature inside the sample holder is the same as the external temperature. If the temperature was allowed to equilibrate it would be expected that the temperature inside the sample holder would be higher than the outside temperature due to radiative cooling since safety considerations prevented allowing sufficient time for equilibration to occur. It is very possible that the internal temperature of the sample holder was lower than the external temperature. The BN crucible was necessary, as it was found that Ta and Pt will react to form a Ta-Pt

alloy, that melts at temperatures below the melting point of Pt. An Al catcher foil was positioned above the sample holder to catch or trap the released activity.

Two identical experiments were carried out. As in the Au work initial gamma spectra of the Pt samples, (small pieces of a Pt target), were collected. The samples were wrapped in the sample holders and a small hole was made in the Ta foil above the opening of the crucible to allow volatile species to escape. The sample holder was firmly clamped between the copper electrodes and the entire system evacuated to a pressure of <50 mtorr. The temperature was raised to either an external temperature of >1770°C or until the power cables to the copper electrodes became too hot. If the current was raised too high the power cables would begin to smoke and break down, clearly an unsafe condition. This would occur at a temperature of ≈1700°C. The temperature was held at the maximum value for as long as was deemed safe (≈3-5min) to attempt to allow for equilibration throughout the sample holder. The temperature was lowered and the system was allowed to cool thoroughly under vacuum, then disassembled and gamma spectra of all components were collected.

Despite the use of a high temperature furnace system it was impossible to completely melt the Pt target samples. Partial melting was evident from the physical state of the samples and lead to some useful results. The results were calculated as per the Au work .

Figure 12 - Vacuum evaporator, schematic.

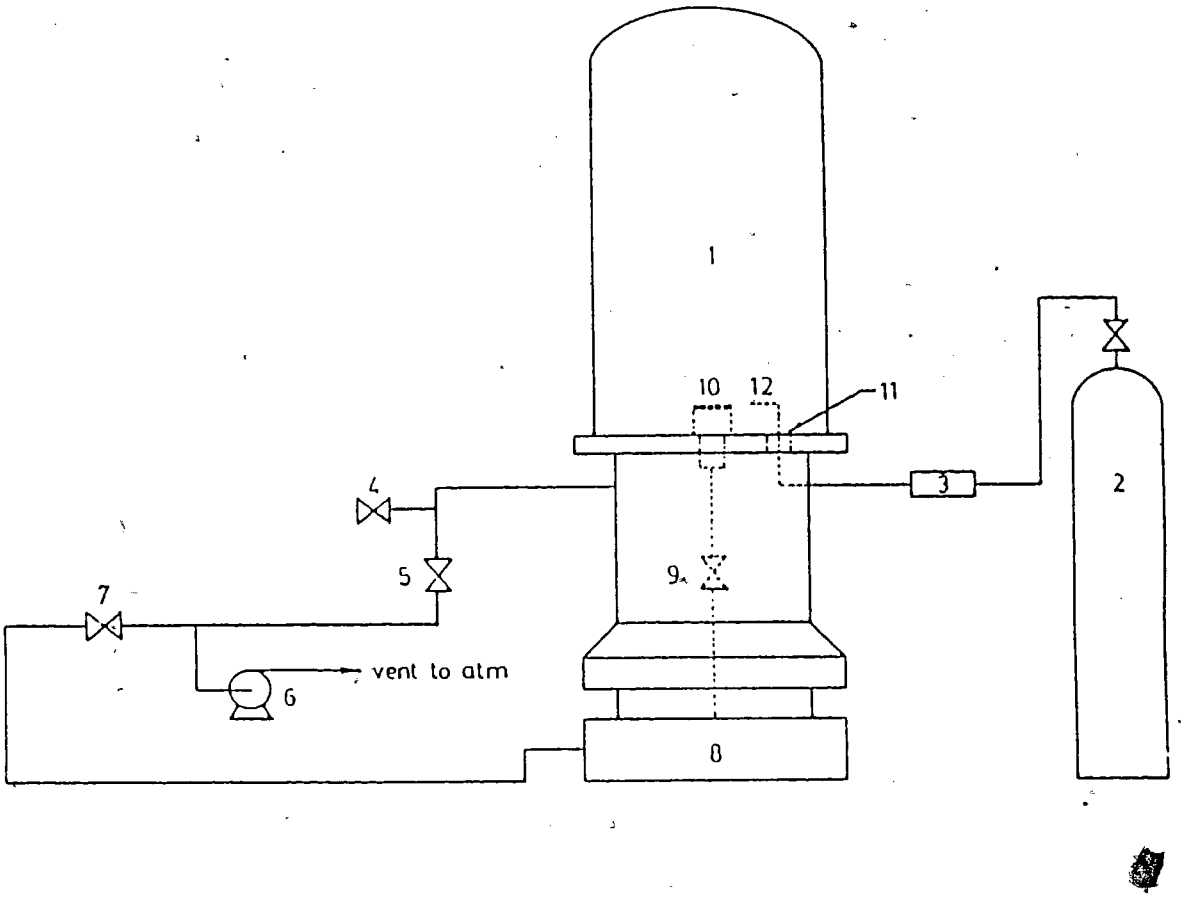

1 EVAPORATOR
2 He/O_2 SUPPLY
3 DIGITAL FLOWMETER
4 AIR RELEASE VALVE
5 ROUGHING VALVE
6 MECHANICAL VACUUM PUMP
7 FORELINE VALVE
8 DIFFUSION PUMP
9 HIGH VACUUM VALVE
10 ELECTRODE (see figure 2)
11 BUSHING (see figure 3)
12 NOZZLE

Figure 13 - Copper electrodes of vacuum evaporator.
1 - Copper electrodes
2 - Tantulum sample holder

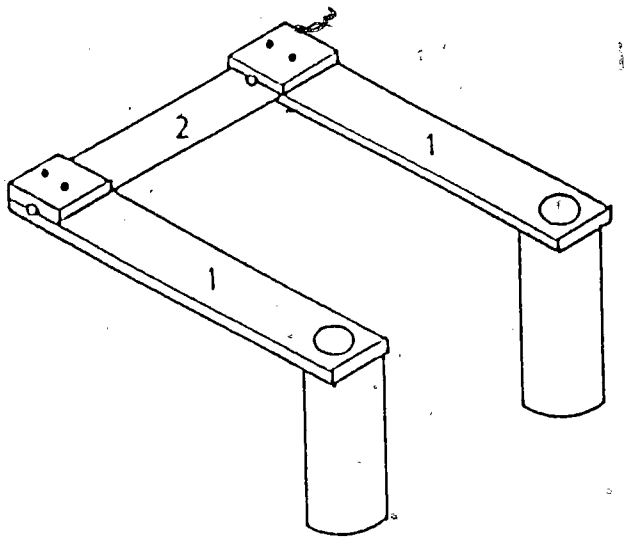

Ir Target

The Ir target was not investigated using this technique for two reasons. Ir has a melting point even higher than that of Pt (2410°C)[24], making it even more difficult to melt than Pt, and is known to react with O_2, even in trace amounts, at elevated temperatures to form volatile oxides, which would lead to destruction of the target material.

RESULTS AND DISCUSSION

^{186}Re Cross-sections

Results for the cross-section for ^{186}Re from an Ir target and upper limits on the cross-sections for ^{186}Re from Au and Pt targets, using two methods, are presented in Tables 8, 9, and 10. Where there is disagreement between the two methods, the upper limit should be taken as the smaller of the two values. It was not possible to determine upper limits using method two for all energies. The method relies on knowing the amount of ^{186}Ir produced. As mentioned previously it was not possible to perform half life analysis for some targets, likewise it was not possible to determine cross-sections or upper limits, using method two, for these targets.

The cross-section for ^{186}Re from an Ir target is the first reported value for this reaction, Ir(p,x)^{186}Re. This result is given credibility by the agreement of cross-sections for other isotopes from the Au target with literature values, which are discussed later.

The errors on this result arise mainly from the literature value of the cross-section for ^{24}Na used in determining the proton flux (±6.5%)[42] and in determining the areas of the gamma peaks. Errors for all cross-sections were determined using standard methods of propagation of errors[49]. Included in the error determination were errors on the total

Table 8

CROSS-SECTIONS FOR ^{186}Re, Ir TARGET

Energy MeV	Cross-section σ (mb)	SILT estimate (mb)
500	4.3 ± 0.6	6.0

Table 9

CROSS-SECTION UPPER LIMITS FOR ^{186}Re, Au TARGET

Energy MeV	Upper-Limit Method 1 σ (mb)	Upper-Limit Method 2 σ (mb)	SILT estimate	
			MeV	mb
235	0.17 (2)*	0.31	200	0.71
290	0.42	1.23	300	1.07
370	0.56	0.76	400	1.45
445	0.67	0.11		
500	0.68	0.09	500	1.71

Table 10

CROSS-SECTION UPPER LIMITS FOR ^{186}Re, Pt TARGET

Energy MeV	Upper-Limit Method 1 σ (mb)	Upper-Limit Method 2 σ (mb)	SILT estimate	
			MeV	mb
235	0.20	2.2	200	7.97
290	0.64	——	300	10.15
370	0.76	0.12	400	13.15
500	0.60	——	500	15.12

* This result is the average of two target irradiations.

number of protons, (including error on ^{24}Na cross-section), errors on target mass and area, errors on A_{EOB} as determined by the half life fitting programs. Other errors such as errors on decay constant, counting intervals, and branching ratios were neglected as they were negligible compared to the major sources of errors.

The upper limits set on the cross-section for ^{186}Re from Au and Pt targets are somewhat lower than expected according to SILT estimates[25,26]. In fact according to the SILT estimates one would expect Pt to have the largest cross-section. Since Ir is closer to Re, in the periodic table, than Au or Pt, one would expect the cross-section for ^{186}Re to be largest for an Ir target. This appears to be the case but does not agree with the SILT predictions. As discussed in Appendix A it is expected that the estimates for the Pt target would be the least accurate, so the disagreement between the experimental and calculated is not unreasonable.

Since the goal of this work was to determine the feasibility of proton spallation as a production method, the results are analysed in terms of the ability to produce quantities of the isotope large enough for patient doses. This was done for the three target materials by estimating the cyclotron time required to produce a single patient dose of 250 mCi, based on the maximum possible production rate. For the Au and Pt targets a best case scenario was assumed by treating the upper limits as actual cross-sections. The maximum production rate is determined by the saturation activity. Saturation activity is defined

as the activity when the rate of production equals the rate of decay, and is dependent on the cross-section for production. If the products of a nuclear reaction are stable, then the number of product atoms produced during a bombardment of time t is equal to;

$$N = N_t * \sigma * I * t \qquad (4)$$

N_t = Target thickness (atoms/cm^2)

σ = Cross-section (cm^2)

I = Proton current (p/s μA)

t = Bombardment time (s)

If however the products are radioactive, then it is possible that some of the product nuclei will decay during the irradiation. If the bombardment of the target lasts long enough, eventually the rate of production will equal the rate of decay and saturation activity will be reached and is equal to;

$$P\lambda = N_t * \sigma * I \qquad (5)$$

$P\lambda$ = Saturation activity

If the bombardment does not last long enough to reach saturation, the activity at the end of bombardment (EOB) is given by;

$$P\lambda = N_t * \sigma * I * (1 - e^{-\lambda t}) \qquad (6)$$

Using these equations the saturation activities have been determined for producing ^{186}Re from Au, Pt, and Ir. The saturation activities and irradiation times that would be required to produce a patient dose of 250 mCi for specific beam currents and target thicknesses are presented in Table 11. The saturation activity for Au is such that it is impossible to produce 250mCi of ^{186}Re with a target thickness of 10 g/cm^2 and a beam current of 100 μ. The beam current that can be used depends on the facility. TRIUMF can deliver a maximum beam current of $\approx$100 μA, while some facilities such as Los Alamos can deliver up to 1mA[22]. The largest reasonable target thickness that can be used is $\approx$100 g/cm^2. Given the energy ranges of protons in Au, Pt and Ir[50], this thickness results in a 30% energy degradation of a 500 MeV proton beam. Thus with optimal beam currents and a target thickness of 100 g/cm^2 the minimum irradiation time required at TRIUMF would be $\approx$90 hours for an Au target.

TABLE 11

Estimates of cyclotron time required to produce a single patient dose, 250 mCi, of ^{186}Re from Au, Pt, and Ir targets.

Target	Cross-Section (mb) 500 MeV	Saturation Activity mCi/μA•g/cm^2	t(hr) 100μA, 10g/cm^2	t(hr) 100μA, 100g/cm^2	t(hr) 1mA, 100g/cm^2
Au	≈0.09	0.05	—	90	6.7
Pt	≈0.6	0.3	234	11	1.1
Ir	4.3	2.2	16	1.5	0.15

It must be emphasized that this is an absolute minimum irradiation time for the production of ^{186}Re: the cross-section used in the calculation is only an upper limit; the actual cross-section could be a factor of 2, 10, 100 or even smaller. Also, no allowances have been made for the time required for separation and preparation of the radiopharmaceutical. This would probably require the irradiation time to be increased by a factor of ≈2, allowing one half life (90 hours) for processing time. Hence Au and Pt targets would probably require very long irradiation times to produce a patient dose of 250mCi, or it may be impossible to ever reach the desired activity, as is the case with a 10 g/cm^2 Au target. Clearly the irradiation times required for the Au and Pt targets are prohibitive. For the Ir target, the cross-section used for the calculation is a measured cross-section rather than an upper limit. Correcting for processing time would increase the irradiation time by a factor of 2, allowing for one half life for separation and preparation of the radiopharmaceutical. The resulting minimum irradiation time is then ≈3 hours. This irradiation time is feasible. However the problems that may be encountered in working with such a thick target, and the ensuing separation problems may reduce the feasibility of this approach. A 100 g/cm^2 target, if using the same area as in this work (6.25 cm^2) would be approximately 5 cm thick and weigh between 600 and 700 g, depending on the target. This mass is significant and may cause some difficulties in separation.

Since Ir forms oxides in the presence of O_2, the simple separation procedure available for separating Re from Au and Pt is not applicable to Ir targets. More important would be the levels of radioactivity present in the target. Remote handling facilities are required, the target may have to be allowed to cool before handling which would increase further the processing time. Also to be considered is the availability of a high energy proton accelerator. There are very few of these machines in operation and all are in high demand for many areas of research. They do not have the accessibility of the low energy cyclotrons. However, this approach does have merits, and future studies should focus on developing a separation technique for separating Re from Ir that can be carried out remotely and allows for recovery of the target material.

Cross-sections of Ir, Os, Re, and Pt Isotopes

Results for cross-sections of Ir, Os, Pt, and other Re isotopes are compiled in Tables 12 and 13 along with literature values[28,29]. Two sets of literature values are available for the spallation of Au but no literature values were found for the spallation of either Pt or Ir targets. Table 14 details the gamma energies and intensities that were used throughout the calculations.[27] Tables 15 and 16 detail the cross-sections that were calculated for each gamma energy, and the reported value for comparison. The results presented in the tables were arrived at by averaging individual results found using various gamma peaks and half life fits. In many cases the half life fits were not ideal due to small data sets. Therefore more than one fitted set of data was used for each gamma peak analysed, and if possible fitted data from both the CLSQ[45] program and the FRANTIC[46] program were used. The results in Tables 15 and 16 were averaged for each gamma energy. Since in many cases more than one calculation was completed for each gamma energy, the reported value is not necessarily the average of the values in Tables 15 and 16. The reported value was averaged over all calculated values.

In determining the half life fits, half lives were both, held constant and allowed to vary, and the best fits were used in the calculations. Errors were determined for each individual result using standard methods of propagation of errors[49]. Relative errors were determined by the square root of the sum of the squares of individual relative errors. For example;

$$\text{if } Z = X * Y \tag{7}$$

$$\Delta Z = Z * ((\Delta X/X)^2 + (\Delta Y/Y)^2)^{\frac{1}{2}} \tag{8}$$

Determining cross-sections for isotopes other than ^{186}Re serves two purposes. It provides confirmation of previously published results and, in doing so, provides a means of verifying this work.

TABLE 12

CROSS-SECTIONS FOR Ir, Os, Re, and Pt ISOTOPES, Au TARGET and REFERENCE VALUES
All isotopes are ground state, type indicates cummulative (C) or independent (I) cross-sections.

Au TARGET CROSS-SECTIONS

Isotope	Type	Cross-Section in mb at proton energy (MeV)				
		235	290	370	445	500
^{186}Ir	C	39.6±7.8	49 ± 19	42.6±14.4	35.7±7.0	28.0±5.1
^{189}Ir	C	81.5±9.9		94 ± 17		60.7±3.5
^{190}Ir	I		4.1±0.5	5.2±0.8		4.1±0.6
^{182}Os	C	37.3±8.9	34 ± 1	66 ± 18	53.1±7.4	47 ± 10
^{183}Os	C				47.7±8.8	
^{185}Os	C	78.7±6.9	107 ± 12	106.3±4.0	71.2±5.7	59.0±1.8
^{191}Os	C		8.0±0.3	11.9±1.4		7.8±1.4
^{181}Re	C	30.0±4.5		67.3±5.9	57.9±9.2	53.3±10.0
^{182}Re	C	2.0±0.2			4.8±0.4	3.6±1.1
^{183}Re	C			41.3±3.3		66.4±9.5
^{184}Re	I		7.0±0.4	2.5±0.3		
^{188}Pt	C	59.6±8.5	101 ± 13	66 ± 19		49.2±8.9

REFERENCE CROSS-SECTIONS

Isotope	Type	Kaufman σ (mb)		Asano σ (mb)
		200 MeV	490 MeV	500 MeV
^{186}Ir	C			20 ± 1
^{189}Ir	C	85 ± 7	57 ± 4	52 ± 6
^{190}Ir	I	2.74±0.25	4.5±0.4	2.1±0.1
^{192}Ir	I	1.22±0.15	2.18±0.22	1.6±0.1
^{182}Os	C	24.1±2.2	55 ± 5	35 ± 6
^{183}Os	C			15 ± 3
^{185}Os	C	71 ± 6	70 ± 6	61 ± 5
^{191}Os	C			2.9±0.7
^{181}Re	C	19.7±1.8	60 ± 5	46 + 3
^{182}Re	C			84 ± 13
^{183}Re	C	33.5±2.9	60 ± 5	47 ± 7
^{184}Re	I			47 ± 8
^{188}Pt	C	98 ± 7	57 ± 3	41 ± 7

TABLE 13

Cross-sections for Ir, Os, Re, and Pt isotopes, Pt and Ir targets
Type indicates whether cross-section is cummulative (C) or independent (I).

Isotope	Type	σ in mb at proton energy (MeV)		
		Pt-235	370	Ir-500
^{186}Ir	C	54.5±8.1	38.9±9.3	25.0±6.8
^{189}Ir	C	83.5±10.5	25.8±2.2	39 ± 4
^{190}Ir	I	15.7±2.0	6.1±0.8	45.2±3.4
^{192}Ir	C	13.5±3.4	4.4±0.3	43.7±1.5
^{182}Os	C	52.0±6.6	62.0±3.0	42.6±3.5
^{185}Os	C	73.6±11.5	24.5±4.5	
^{191}Os	C		1.5±0.8	14.0±0.8
^{181}Re	C	46.7±7.2	51.6±10.0	59.4±5.2
^{182}Re	C	2.0±0.7	1.7±0.7	10.1±2.9
^{183}Re	C		23.3±3.6	90 ± 9
^{184}Re	I		7.6±1.1	
^{186}Re	I			4.3±0.6
^{188}Pt	C	84 ± 17	22.7±3.3	

Table 14 - List of gamma energies and intensities used for cross-section calculations.

Isotope	Gamma Energy (keV)	Intensity (γ/100 transitions)
^{186}Ir	137.2	41.3
	296.8	62.3
	434.8	33.8
	584.4	5.37
^{189}Ir	244.9	6.0
^{190}Ir	186.7	48.2
	361.1	12.6
	371.2	22.0
	407.2	27.5
	518.6	32.8
	558.0	29.0
	569.3	27.5
	605.1	38.5
^{192}Ir	295.9	28.7
	308.4	29.7
	316.5	82.9
	468.1	48.1
	604.4	8.33
^{182}Os	130.8	3.52
	180.2	36.8
	263.3	6.98
^{183}Os	114.4	20.8
	851.0	3.9
^{185}Os	646.1	80.8
	717.5	4.11
	874.8	6.59
	880.5	4.98
^{191}Os	129.4	25.7
^{181}Re	360.7	12.0
	365.5	56.4
	639.0	6.43
^{182}Re	169.2	12.2
	222.1	9.21
	229.3	27.9
	256.4	10.3
	276.3	9.49
	339.3	6.03
^{183}Re	162.3	23.5
	208.8	2.99
	291.7	3.18
^{184}Re	894.8	15.6
^{186}Re	137.2	9.2
^{188}Pt	155.0	35.9
	478.0	17.8
	633.0	22.0
	829.4	6.22

Table 15 - Cross-sections as a function of gamma energy and proton energy. Au target.

Isotope	Gamma energy (keV)	Cross-section in mb at proton energy (MeV)				
		235	290	370	445	500
^{186}Ir	137.2	23.3	18.8	34.2	29.1	23.2
	296.8	44.8	34.0			33.6
	434.8	42.9	47.7	56.4	42.5	30.9
	584.4	38.5	65.7	44.5	38.8	
	This Report	39.6	49	42.6	35.7	28.0
^{189}Ir	244.9	81.5		94		60.7
	This Report	81.5		94		60.7
^{190}Ir	371.2		4.4	4.4		3.7
	407.2		3.5			3.5
	518.6					5.0
	558.0		4.3	6.2		5.1
	569.3		4.4	5.8		4.2
	605.1		4.9	5.1		4.0
	This Report		4.1	5.2		4.1
^{182}Os	130.8			47.2		42.3
	180.2	37.3		68.0	48.7	39.7
	263.3		34	81.5	61.9	55.8
	This Report	37.3	34	66	53.1	47
^{183}Os	114.4				37.5	
	851.0				62.9	
	This Report				47.7	
^{185}Os	646.1	78.7	101.2	102.9	71.2	58.1
	717.5		106.4			
	874.8		97.8			51.8
	880.5		124.4	109.4		61.9
	This Report	78.7	107	106.3	71.2	59.0
^{191}Os	129.4		8.0	11.9		7.8
	This Report		8.0	11.9		7.8
^{181}Re	360.7	32.7		68.9		64.2
	365.5	28.6		68.8		55.2
	639.0			62.5	57.9	39.4
	This Report	30.0		67.3	57.9	53.3
^{182}Re	169.2	2.0				
	222.1					3.1
	229.3					4.4
	256.4				4.8	2.8
	This Report	2.0			4.8	3.6
^{183}Re	162.3			41.3		65.4
	208.8					75.2
	291.7					59.4
	This Report			41.3		66.4
^{184}Re	894.8		7.0	2.5		
	This Report		7.0	2.5		
^{188}Pt	155.0	53.8	74.8	57.8		39.8
	478.0	72.2	112.2	67.3		57.0
	633.0	67.5	105.8	59.3		56.6
	829.4	68.6	96.9	78.9		54.4
	This Report	59.6	101	66		49.2

Table 16 - Cross-sections as a function of gamma energy and proton energy. Pt and Ir targets.

Isotope	Gamma energy (keV)	Cross-section in mb at proton energy (MeV)				
		Pt	235	370	Ir	500
^{186}Ir	137.2			36.0		24.7
	296.8		68.7			
	434.8		48.7	44.8		25.8
	584.4		53.2			
	This Report		54.5	38.9		25.0
^{189}Ir	244.9		83.5	25.8		39
	This Report		83.5	25.8		39
^{190}Ir	186.7		15.7	7.8		38.9
	361.1			5.3		45.8
	371.2			5.8		44.3
	407.2					42.9
	518.6			5.8		44.4
	558.0			7.1		50.5
	569.3			6.2		47.8
	605.1					46.6
	This Report		15.7	6.1		45.2
^{192}Ir	295.9		16.3			
	308.4		9.8	4.6		
	316.5		13.8	4.2		42.4
	468.1		11.5			44.7
	This Report		13.5	4.4		43.7
^{182}Os	130.8			61.6		
	180.2		52.0	44.8		41.1
	263.3			74.7		44.7
	This Report		52.0	62.0		42.6
^{185}Os	646.1		79.5	21.8		
	874.8			24.2		
	880.5		61.8	28.3		
	This Report		73.6	24.5		
^{191}Os	129.4			1.5		14.0
	This Report			1.5		14.0
^{181}Re	360.7					55.9
	365.5		45.5	52.4		62.8
	639.0		49.1	49.8		58.4
	This Report		46.7	51.6		59.4
^{182}Re	169.2			1.1		
	222.1			2.3		14.3
	229.3			1.6		12.0
	256.4		2.0	1.2		7.3
	276.3			2.5		9.3
	339.3					8.9
	This Report		2.0	1.7		10.1
^{183}Re	162.3			22.8		90
	208.8			24.7		
	291.7			23.3		
	This Report			23.3		90
^{184}Re	894.8			7.6		
	This Report			7.6		
^{186}Re	137.2					4.3
	This Report					4.3
^{188}Pt	155.0		66.5	18.0		
	478.0		96.3	25.2		
	633.0		77.5	25.2		
	829.4		78.1	22.5		
	This Report		84	22.7		

When individual results were averaged for the final reported result, errors were determined either by calculating the standard deviation of the averaged values, or by propagation of individual errors. The standard deviation was calculated only if there were six or more values to be averaged. Overall most errors were within ±10%, the majority of this arising from the error on the ^{24}Na cross-section and the remainder arising from peak areas and half life fits. These errors are reasonable and indicate the results are quite good considering the limited amount of data available.

By comparing the experimentally determined cross-sections with the SILT estimates in Tables 3a and 3b it is possible to see that the SILT estimates calculate independent rather than cummulative cross-sections. This is illustrated by the results and estimates for ^{189}Ir and ^{190}Ir and for ^{183}Re and ^{184}Re, two pairs of isotopes where the large difference between a cummulative and independent cross-section is obvious. The SILT estimates do not show this large difference, while the experimental results do. This means that the difference observed between the estimated cross-sections for ^{186}Re and the calculated upper-limits is not due to the estimations determining cummulative rather than independent cross-sections. There must be an inadequacy in the estimations for products that are very close to the target mass.

Au Target

There is some disagreement between the two sets of literature values of Kaufman[28] and Asano[29], in most cases the present results have a better agreement with the results of Kaufman.

Isotopes for which there is disagreement between the two sets of published results include ^{190}Ir, ^{182}Os, ^{181}Re, ^{188}Pt. For ^{190}Ir the present work agrees with Kaufman[28] but not Asano[29]. ^{182}Os and ^{181}Re results agree with both Kaufman and Asano's work but in both cases present values are closer to those of Kaufman. In the case of ^{188}Pt the present result agrees with both values and lies approximately midway between the two.

There are also some isotopes for which only Asano[29] has reported cross-sections. The present results in most cases do not agree with those of Asano. The closest agreement exists for ^{186}Ir; although not within reported errors the results are reasonably close. The results for ^{183}Os, ^{191}Os, ^{182}Re, and ^{184}Re however are dramatically different. With the exception of ^{183}Os the current results are reported for either two or three energy values and follow consistent trends over the different energies. This coupled with the fact other results have had better agreement with Kaufman's work lends more credibility to the present work over that of Asano.

One difficulty encountered while comparing results is that one does not know the gamma energies that were used in the calculations for the literature values. For example, the results for ^{182}Re were derived from three peaks and were consistent for the three gamma's and over three energies. In determining which gammas could be used to calculate cross-sections the main criteria was half life. However if one peak gave significantly different results the peaks were checked for the appropriate relative intensities. The experimental peak areas should agree with the literature values of relative intensities for the gamma emissions. One case where this occurred was for ^{190}Ir. ^{190}Ir exhibits at least eight characteristic gamma energies in intensities large enough to be easily observed. In many cases, for the Au targets, two of these gammas did not exhibit the correct relative intensity while the other six did. These two that did not agree also led to cross-sections that did not agree and were not included in the reported results. If only one or two gamma energies had been used for the calculations it is possible that this difference would not be noticed, and would result in inaccurate results.

Pt and Ir Targets

The results for the Pt and Ir targets are difficult to discuss as there are no published values for comparison. These results must stand on the basis that since the Au target results were comparable with literature values it is reasonable that the Pt and Ir target results are also credible.

In general it appears that cross-sections for products from the Ir target were greater than those from the Pt target, while those of the Pt and Au targets were comparable.

This work has been instrumental in confirming the results of Kaufman and in doing so lending credibility to the present work, in particular to the cross-sections for ^{186}Re.

SEPARATION RESULTS

Au Target

The results for the separation of Re, Ir, and Os form a Au target are presented in Table 17. Essentially, quantitative release was achieved in both trials for all three elements.

Analysis, by gamma ray spectroscopy, of all components of the quartz insert was instrumental in mapping the distribution of the released activity. Figure 15 shows schematically the general areas where the released activity was observed. Nearly all of the ^{185}Os activity was found around the thermocouple inlet tube, while the ^{183}Re and ^{192}Ir activity was found at the opposite end of the quartz insert near the inlet and outlet gas tubes. It is unclear why the Os activity did not follow the behavior of the Re and Ir activity. One would expect that all three isotopes would follow the same path and condense out according to their condensation temperatures. Negligible activity was observed in either the U-trap or the glass wool trap, and all released activity could be accounted for.

A mapping of released activity was not completed for the second trial as the insert could not be completely cleaned of activity between trials. Cursory observations indicated that most of the activity was deposited in the same areas as for the first trial.

TABLE 17a

SEPARATION RESULTS - Au TARGET

Oven Trial #1

Energy	Activity (cpm)		% Released
	Before melting	After melting	
^{183}Re $t_{\frac{1}{2}}$ = 70 d			
109.7	218	0	100
162.3	1000	0	100
208.8	125.5	0	100
291.7	78	0	100
^{192}Ir $t_{\frac{1}{2}}$ = 73.83 d			
295.9	40	0	100
308.5	46	0	100
316.5	63	0	100
468.1	28	0	100
^{185}Os $t_{\frac{1}{2}}$ = 93.6 d			
646.1	1146	22	98
717.4	62	0	100
874.8	85	0	100
880.5	70	0	100

TABLE 17b

SEPARATION RESULTS - Au TARGET

Oven Trial #2

Energy	Area		% Released
	Before melting	After melting	
^{183}Re $t_{\frac{1}{2}}$ = 70 d			
109.7	142	0	100
162.3	826	0	100
208.8	84	0	100
291.7	73	0	100
^{192}Ir $t_{\frac{1}{2}}$ = 73.83 d			
295.9	40	25	37
308.5	215	0	100
316.5	48	0	100
468.1	19	0	100
^{185}Os $t_{\frac{1}{2}}$ = 93.6 d			
646.1	1230	91	93
717.4	55	0	100
874.8	78	7.5	91
880.5	68	0	100

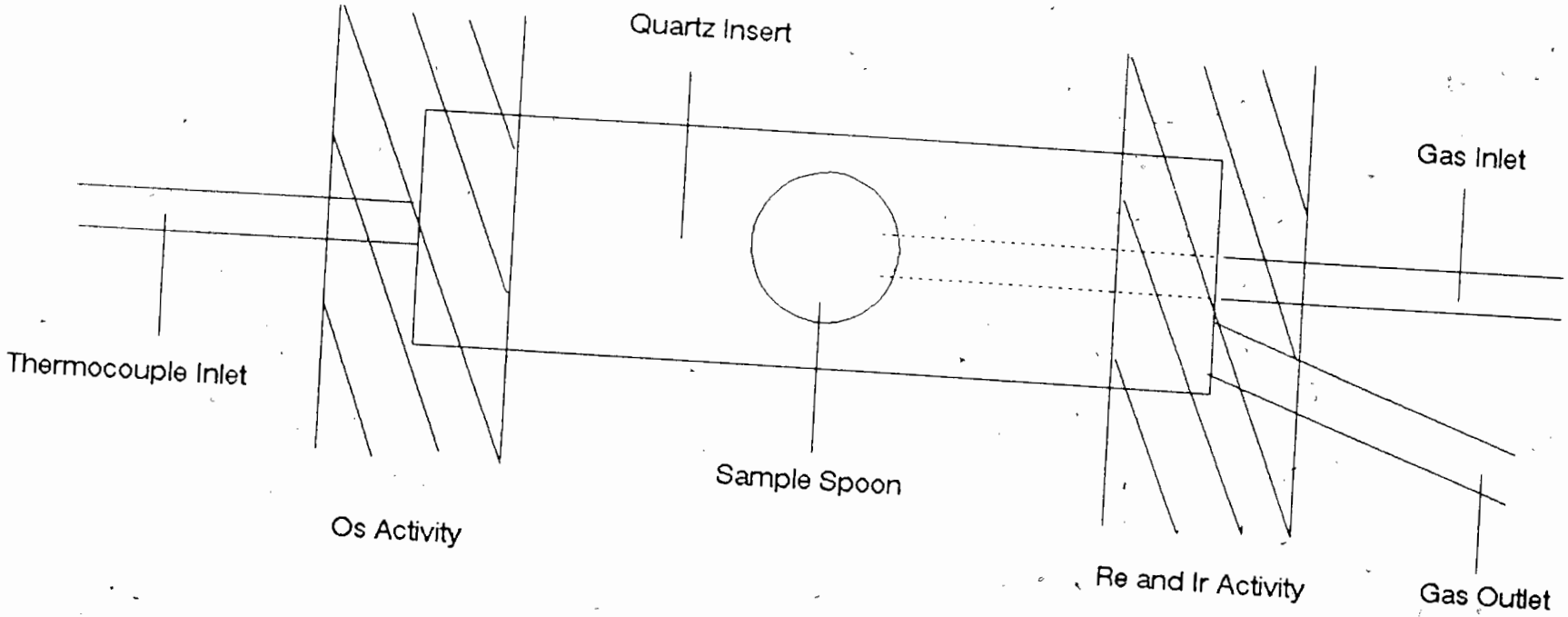

Figure 14 - Distribution of Released Activity

Pt Target

As mentioned previously, difficulties were encountered in attempting to melt the Pt target foil. The Pt sample was not completely melted in either of the experimental trials.

In the first experiment, the foil was visibly disfigured and had obviously started to melt. Analysis of the gamma spectra collected before and after heating showed release efficiencies of between 50 and 100 % for ^{183}Re, ^{192}Ir, and ^{185}Os, see Table 18. There was very little activity remaining in the target foil after heating.

The second experiment was not as successful. The maximum temperature reached was lower than in the first trial, and the only visible change in the target was some disfigurement. Analysis of gamma spectra showed relatively little release. ^{183}Re was released with a 10 - 20 % efficiency, the long lived Ir and Os isotopes were not released to any appreciable extent.

Aside from the target foils, the Ta foil used in the sample holder and the Al catcher foil were also analysed by gamma spectroscopy. No activity was observed for either case. The only part of the sample holder which was not analysed by gamma spectroscopy was the BN crucible used in the sample holder, due to geometry restrictions of the Ge(Li) detector used. It is most likely that the released activity was deposited on the BN crucible or on the walls of the evaporator. BN is a

thermal insulator and was probably slightly cooler than the rest of the sample holder, which could cause the radioactivity to condense on the BN crucible.

TABLE 18a SEPARATION RESULTS - Pt TARGET

Evaporator Trial #1

Energy	Activity (cpm)		% Released
	Before melting	After melting	
^{183}Re $t_{\frac{1}{2}}$ = 70 d			
162.3	72	30.6	58
^{192}Ir $t_{\frac{1}{2}}$ = 73.83 d			
308.5	33.9	0	100
316.5	60.3	28.5	53
468.1	6.6	0	100
^{185}Os $t_{\frac{1}{2}}$ = 93.6 d			
646.1	90.0	46.4	48
874.8	9.1	0	100
880.5	8.0	0	100

TABLE 18b SEPARATION RESULTS - Pt TARGET

Evaporator Trial #2

Energy	Activity (cpm)		% Released
	Before melting	After melting	
^{183}Re $t_{\frac{1}{2}}$ = 70 d			
162.3	554	439	20
291.7	150.5	136	10
^{192}Ir $t_{\frac{1}{2}}$ = 73.83 d			
308.5	72	72	0
316.5	205	207	0
468.1	82	78	0
^{185}Os $t_{\frac{1}{2}}$ = 93.6 d			
646.1	886	944	0
717.4	46.5	46	0
874.8	55	56.5	0
880.5	49	51.5	0

Separation Discussion

The separation work has provided some promising results. It is apparent that this method could be successful for separating Re from the various target materials. The work on the Au target shows that 100% release is obtainable. Although the Pt target work was not as successful, it seems likely, on the basis of the results, that with the use of a suitable furnace system, quantitative release of Re, Ir, and Os isotopes from Pt targets would be possible. This work was limited by the level of equipment available for use, a suitable furnace system should be easily obtainable. The next logical step for this work to follow would be to investigate the isolation of Re using such a separation procedure. This should be a relatively simple task. The basis of this technique is that volatile oxides are formed which allow the Re, Ir, and Os to be released from the target material. The different metallic oxides condense at varying temperatures. The differences are large enough that isobaric separation can be achieved by either a negative temperature gradient (*i.e.* a thermochromatographic column), or a "cold finger" at a known temperature. The cold finger approach would be useful for Re separation as Re oxides are the first of the three to condense, at a temperature of ≈450°C. The Ir oxides do not condense until ≈250°C and the Os oxides at a temperature of < 100°C. Isotopic separation could then be achieved using either an on or off-line mass separator such as the TISOL facility[51].

This separation technique certainly warrants continued investigation. Although Au and Pt targets may not be useful for producing ^{186}Re they may yet have potential for production of other isotopes such as ^{188}Re. This technique could be of use in the production of ^{188}Re and other isotopes for medical or other purposes. It is an advantageous technique since the target material is neither destroyed nor chemically changed during processing and can be used repeatedly, an important point when expensive target materials are used.

SUMMARY AND CONCLUSIONS

1) The cross-section for the production of ^{186}Re from the proton spallation of Ir at 500 MeV was determined to be 4.3 ± 0.6 mb.

2) The cross-sections for the production of ^{186}Re from the proton spallation of Au and Pt targets at energies from 235 to 500 MeV could not be determined; upper limits were set as in Tables 9 and 10.

3) On the basis of the calculated upper limits it was determined that the proton spallation of Au or Pt targets is not a viable production method for ^{186}Re.

4) On the basis of the cross-section for ^{186}Re from an Ir target it was determined that the proton spallation of an Ir target has potential as a production method for ^{186}Re. Future studies should concentrate on developing a separation method for separating Re from an Ir target.

4) Cross-sections for other Re, Ir and Os isotopes were calculated and compared with published values.

5) It was determined that a thermal separation procedure is a viable first step in designing a method for separating Re, Ir, and Os from Au and Pt targets. This procedure warrants further investigation and development.

APPENDIX A

SILT Calculations[25,26]

SILT calculations use the semiempirical equations developed by Silberberg and Tsao. The previously available semiemperical calculations of Rudstam were not applicable for light product nuclei or for cases where the difference between target and product mass, ΔA, is very small. The Silberberg and Tsao equations are based on those of Rudstam but have been corrected so that they are applicable in the regions where the equations of Rudstam were not.

The generalized form of the cross-section equation for the production of a product (Z,A), from a target, (Z_t, A_t), by protons of energy E is:

$$\sigma = \sigma_o \, f(A) \, f(E) \, e^{-P\Delta A} \exp(-R|Z - SA + TA^2|^{\nu})\Omega\eta\xi$$

Where;

σ_o = a normalization factor

$f(A)$ & $f(E)$ = correction factors that correct for products from targets with $Z_t > 30$ and very large ΔA, products that result from fission, fragmentation, and evaporation reactions.

$e^{-P\Delta A}$ = takes into account the decrease in σ with increase in ΔA

$\exp(-R|Z - SA + TA^2|^{\nu})$ = takes into account the distribution of σ for products of various isotopes of an element Z and is related to the statistical nature of evaporation reactions.

Ω = nuclear structure factor

η = nucleon pairing factor

ξ = enhancement factor for light evaporation products.

Variations of this equation are used depending on the target and product masses, and therefore on the type of reaction that best describes the process occurring. Figure A shows the regions of the different processes, and table a describes the various conditions under which the various equations should be used.

The reactions occurring in the production of ^{186}Re from Au, Pt, and Ir targets are as follows:

$$^{197}Au(p,5p11n)^{186}Re$$

$$^{194}Pt(p,4p8n)^{186}Re$$

$$^{195}Pt(p,4p9n)^{186}Re$$

$$^{196}Pt(p,4p10n)^{186}Re$$

$$^{198}Pt(p,4p12n)^{186}Re$$

$$^{191}Ir(p,3p5n)^{186}Re$$

$$^{193}Ir(p,3p7n)^{186}Re$$

According to the conditions in table A and the definition of x_{max};

$$x_{max} = \frac{A_t}{25} + 0.5$$

Both Ir reactions are peripheral reactions, the Au reaction is a spallation reaction, and the Pt reactions particularly ^{194}Pt lie on the border between peripheral and spallation reactions. The calculated cross-sections for the Pt target are expected to be somewhat less accurate due to the fact the reactions are in the boundary regions of spallation and peripheral reactions. This is because no equations have been developed for reactions of the type (p,ypxn) with $y \geq 4$; due to lack of experimental data, this is the type of reaction occurring with the Pt target. The calculations for the Pt target are based on the equations for spallation type reactions which will cause errors as the reactions are not clearly spallation type. The calculations for the Au and Ir

targets should be fairly accurate. Silberberg and Tsao have compared calculated and experimental cross-sections for many different reactions and energies and have come up with the following agreement for spallation and peripheral type reactions;

Spallation $\Delta A \leq 50$ (0.15 - 6 GeV) $\sigma_{calc}/\sigma_{exp} = 1(+1,-0.5)$

Peripheral $Z_t \geq 29$ ($E \geq 0.15$ GeV) $\sigma_{calc}/\sigma_{exp} = 1(+0.5,-0.3)$

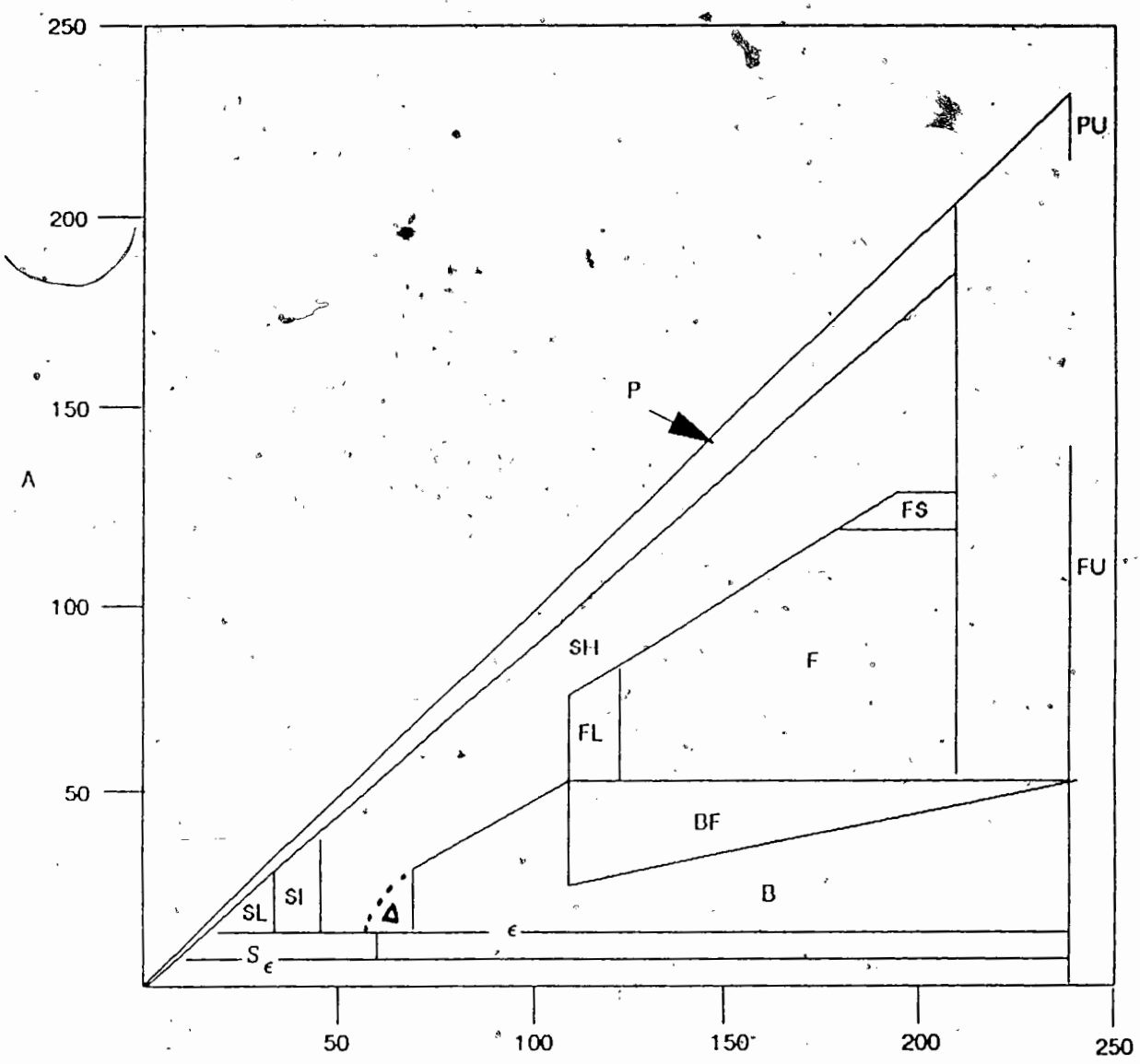

Figure A - Regions of Applicability for various processes. P-Peripheral reactions; PU-Peripheral reactions for uranium; SL, SI, SH- Spallation of light, intermediate, and heavy targets; ϵ-Evaporation; S_ϵ-Combination of spallation and evaporation; F-Fission; FU-Fission of uranium; FL-Fission of light targets with contributions from spallation; FS-Region intermediate to fission and spallation; B-Nuclear breakup reactions; BF-Combination of nuclear breakup and fission; subregion Δ-transition area between domains SH and B.[26]

Table A - Summary of Conditions for the use of Various Cross-section Equations.[26]

Target A,Z	Product A,Z	Conditions				Applicable Cross-section
$A_t = 238$ $Z_t = 92$	$88 \le Z \le 92$ $A \ge 57$; $Z \le 62$ $0.23A_t < A \le 56$ $A \le 0.23A_t$; $Z > 4$ $A \ge 6$; $Z \le 4$					σ_{PU} σ_{FU} $(\sigma_B, \sigma_{FU})_{max}$ σ_{B*} σ_ϵ
$110 \le A_t \le 209$	$A \ge 57$	$\Delta\lambda_c(E_o) - \Delta\lambda \ge 20$	$x \le x_{max}$			σ_P
			$x > x_{max}$	$N/Z \le (N/Z)_c$		σ_S
			$A_t > 125$		$Z > 57$	$\sigma_F^{1-\gamma}\sigma_S^{\gamma}$
		$\Delta\lambda_c(E_o) - \Delta\lambda < 20$		$N/Z > (N/Z)_c$	$53 \le Z \le 57$	$(\sigma_F, \sigma_S)_{max}$
			$A_t \le 125$		$Z < 53$	
	$0.23A_t < A \le 56$ $A \le 0.23A_t$; $Z > 4$ $A \ge 6$; $Z \le 4$					$(\sigma_B, \sigma_F)_{max}$ σ_B σ_ϵ
$69 \le A_t \le 109$	$Z > 4$	$\Delta\lambda \le \Delta\lambda_c(E_o)$	$x \le x_{max}$			σ_P σ_S
			$x > x_{max}$			σ_B
	$A \ge 6$; $Z \le 4$	$\Delta\lambda \le \Delta\lambda_c(E_o)$				σ_ϵ
$A_t \le 68$ $Z_t \ge 29$	$Z \ge 6$		$x \le x_{max}$			σ_P σ_S
			$x > x_{max}$			$\langle\sigma_S, \sigma_\epsilon\rangle$
	$Z = 5$ $A \ge 6$; $Z \le 4$					σ_ϵ

* σ_B and σ_ϵ also apply to the interval $209 < A_t < 238$.

APPENDIX B

Derivation of Beam Integration and Cross-section Equations[18]

The activity present after a bombardment of time t_b is;

$$\frac{dN}{dt} = N_o\lambda = N_t\sigma\phi(1-e^{-\lambda t_b})$$

At time t after bombardment the activity present is equal to:

$$\frac{dN}{dt} = \lambda N = \lambda N_o e^{-\lambda t}$$

Therefore:

$$\frac{dN}{dt} = N_t\sigma\phi(1-e^{-\lambda t_b})e^{-\lambda t}$$

The actual activity present is not what is observed due to branching ratios and the efficiency of the detection system. Observed activity is related to actual activity with the following equation:

$$Y = \frac{dN}{dt} * \epsilon * b$$

Therefore

$$\frac{dN}{dt} = \frac{Y}{\epsilon\ b}$$

and:

$$\frac{Y}{\epsilon\ b} = N_t\sigma\phi(1-e^{-\lambda t_b})e^{-\lambda t}$$

Solving for ϕ and σ gives:

$$\phi = \frac{Y}{\epsilon b N_t \sigma (1-e^{-\lambda t_b}) e^{-\lambda t}}$$

$$\sigma = \frac{Y}{\epsilon b N_t \phi (1-e^{-\lambda t_b}) e^{-\lambda t}}$$

If the counting rate is corrected to end of bombardment time (EOB) as is done by the half life fitting programs used:

$$Y_{EOB} = \frac{Y}{e^{-\lambda t}}$$

and:

$$\phi = \frac{Y_{EOB}}{\epsilon b N_t \sigma (1-e^{-\lambda t_b})}$$

$$\sigma = \frac{Y_{EOB}}{\epsilon b N_t \phi (1-e^{-\lambda t_b})}$$

If $t_{\frac{1}{2}}$ of the isotope in question (eg ^{24}Na or ^{186}Re) is much larger that the bombardment time the following approximation is valid:

$$\text{if } t_{\frac{1}{2}} >> t_b \text{ then } (1 - e^{-\lambda t_b}) \approx \lambda t_b$$

Substituting this into the equations for ϕ and σ gives:

$$\phi = \frac{Y_{EOB}}{\epsilon b N_t \sigma \lambda t_b}$$

$$\sigma = \frac{Y_{EOB}}{\epsilon b N_t \phi \lambda t_b}$$

The activity produced by the half life fitting programs has already been corrected for detector efficiency:

$$A_{EOB} = \frac{Y_{EOB}}{\epsilon}$$

Which leads to:

$$\sigma = \frac{A_{EOB}}{b N_t \phi \lambda t_b}$$

The total number of protons Φ equals:

$$\Phi = \phi t_b$$

Which leads to:

$$\Phi = \frac{Y_{EOB}}{\epsilon b N_t \sigma \lambda}$$

$$\sigma = \frac{A_{EOB}}{bN_t \Phi \lambda}$$

Which are the final equations used for calculating total number of protons and cross-sections throughout.

List of Symbols and their meanings:

N = number of product nuclei

$\frac{dN}{dt}$ = decay rate (activity)

λ = decay constant

t_b = bombardment time

N_t = target thickness (atoms/cm^2)

ϵ = detector system efficiency

b = branching ratio

σ = cross-section

Y = observed counting rate

Y_{EOB} = observed counting rate corrected to EOB

A_{EOB} = activity at EOB

ϕ = proton flux

Φ = total number of protons

APPENDIX C

Sample Calculation of Cross-sections

Ir target, 137.2 keV gamma, ^{186}Re and ^{186}Ir

1) Data corrected for counting intervals and detector efficiency

T1(min)	T2(min)	T3(min)	Area	ϵ	A_{corr}	dpm
2193	36.45	2211.225	74442	1.335E-3	55761797	1529816.0
3504	60	3534	48347	1.335E-3	36214981	603583.0
4871	60	4901	19735	1.335E-3	14782771	246379.5
7953	120	8013	2272	1.335E-3	1701872	14182.27
10483	120	10543	3181	1.335E-3	2382771	19856.42

Where;

T1 = time form EOB to data collection (minutes)

T2 = counting interval (minutes)

T3 = T1 + ½T2 (minutes)

Area = fitted area found from either GXL or GAMANAL

ϵ = detector efficiency

A_{corr} = Area/ϵ

dpm = A_{corr}/T2

2) Following are the CLSQ output files.

IR-137

NP= 5 NC= 2 NV=0 CNV=0.05 BGD= 0.00 SBGD= 0.00

	HALF LIFE	SIGMA H	CPM AT END	SIGMA	DECAY FACTOR
COMP(1)	15.800H	0.000H	0.7316E+07	0.2445E+05	0.5037E+01
COMP(2)	90.600H	0.000H	0.5261E+04	0.3342E+03	0.1326E+01

FIT= 78.023

T(I)	F(I)	FCALC(I)	V(I)	SIGMAF(I)	RATIO(I)
0.2211E+04	0.1530E+07	0.1456E+07	0.7343E+05	0.7649E+04	9.60
0.3534E+04	0.6036E+06	0.5555E+06	0.4808E+05	0.3018E+04	15.93
0.4901E+04	0.2464E+06	0.2060E+06	0.4034E+05	0.1232E+04	32.75
0.8013E+04	0.1418E+05	0.2278E+05	-0.8594E+04	0.1191E+03	-72.16
0.1054E+05	0.1986E+05	0.4655E+04	0.1520E+05	0.1409E+03	107.87

DATA POINTS REJECTED(1) ARE GIVEN BELOW.

BAD T	BAD F
0.8013E+04	0.1418E+05

REPEAT CALCULATION WITHOUT THESE POINTS.

IR-137

NP= 4 NC= 2 NV=0 CNV=0.05 BGD= 0.00 SBGD= 0.00

	HALF LIFE	SIGMA H	CPM AT END	SIGMA	DECAY FACTOR
COMP(1)	15.800H	0.000H	0.7513E+07	0.2449E+05	0.5037E+01
COMP(2)	90.600H	0.000H	0.6349E+05	0.5454E+03	0.1326E+01

FIT= 2.498

T(I)	F(I)	FCALC(I)	V(I)	SIGMAF(I)	RATIO(I)
0.2211E+04	0.1530E+07	0.1540E+07	-0.9750E+04	0.7649E+04	-1.27
0.3534E+04	0.6036E+06	0.6075E+06	-0.3945E+04	0.3018E+04	-1.31
0.4901E+04	0.2464E+06	0.2427E+06	0.3678E+04	0.1232E+04	2.99
0.1054E+05	0.1986E+05	0.1992E+05	-0.6821E+02	0.1409E+03	-0.48

ALL DATA POINTS OK.

IR-137

NP= 4 NC= 2 NV=1 CNV=0.05 BGD= 0.00 SBGD= 0.00

ITERATIONS PERFORMED= 3 CONVERGENT

	1ST COMP	2ND COMP	3RD COMP	4TH COMP	5TH COM
D	0.721808E-03				
DELTA(1)	-0.961068E-05				
DELTA(2)	0.249256E-06				
DELTA(3)	0.187611E-08				
SIGMA	0.315028E-05				

	HALF LIFE	SIGMA H	CPM AT END	SIGMA	DECAY FACTOR
COMP(1)	16.005H	0.070H	0.7287E+07	0.3405E+05	0.4934E+01
COMP(2)	90.600H	0.000H	0.6235E+05	0.6726E+03	0.1326E+01

FIT= 1.921

T(I)	F(I)	FCALC(I)	V(I)	SIGMAF(I)	RATIO(I)
0.2211E+04	0.1530E+07	0.1524E+07	0.5709E+04	0.7649E+04	0.75
0.3534E+04	0.6036E+06	0.6082E+06	-0.4666E+04	0.3018E+04	-1.55
0.4901E+04	0.2464E+06	0.2453E+06	0.1060E+04	0.1232E+04	0.86
0.1054E+05	0.1986E+05	0.1987E+05	-0.9398E+01	0.1409E+03	-0.07

3) Calculation of cross-section, based on the 137.2 keV gamma ray. Using the following formula and the CLSQ results the following cross-sections were calculated.

$$\sigma = \frac{A_{EOB}}{N_t * b * \Phi * \lambda}$$

^{186}Ir	^{186}Re
19.96 ± 2.02 mb	4.34 ± 0.44 mb
19.36 ± 1.96 mb	4.26 ± 0.44 mb

4) Reported value of cross-sections

As the 137.2 keV gamma is the only one available for ^{186}Re these two results are averaged and the error determined as follows:

$$\text{Average} = (4.34 + 4.26)/2$$

$$= 4.30 \text{ mb}$$

$$\text{Error} = \text{Average } ((0.44/4.34)^2 + (0.44/4.26)^2)^{\frac{1}{2}}$$

$$= \pm 0.60 \text{ mb}$$

The results for ^{186}Ir were combined with similar calculations done for gamma energies of 296.8 keV and 434.8 keV, as there were more than six results to average the error was taken to be the standard deviation. Following are the results that were averaged and the final result:

23.1 mb

28.6 mb

19.4 mb

20.0 mb

19.4 mb

20.0 mb

22.1 mb

32.0 mb

40.2 mb

$\sigma = 25.0 \pm 6.8$ mb

REFERENCES

1. Lederer, C.M., Shirley, V.S., Eds., Table of Isotopes, 7th Ed., John Wiley and Sons, 1978.

2. Sinma, K., Yamasali, F., "Letter to the Editor", Phys. Rev. 55, (1939), 320.

3. Smathers, J.B., Myers, L.T., "Use of cyclotrons in medical research: past, present, future.", N.I.M., B10/11, (1985), 1111-1116.

4. Hnatowich, D.J., Layne, W.W., et al, "Radioactive labeling of antibody: a simple and efficient method.", Science, 220, (1983), 613-615.

5. Scheinberg, D.A., Strand, M., Gavson, O.A., "Tumor imaging with radioactive metal chelates conjugated to monoclonal antibodies.", Science, 215,(1982), ~~1511~~ 1513.

6. Fritzberg, A.R., "Advances in ^{99m}Tc-labeling of antibodies.", Nucl. Med. 1987:26:7-12.

7. Spencer, R.P., "Short lived radionuclides in therapy.", Nucl. Med. Biol. 14(6),1987,537-538.

8. Quadri, S.M., Wessels, B.W., "Radiolabeled biomelocules with ^{186}Re: potential for radioimmunotherapy.", Nucl. Med. Biol. 13(4),1986, 447-51.

9. Deutsch, E., Libson, K., Vanderheyden, J.L., Ketring, A.R., Maxon, H.R., The chemistry of rhenium and technetium as related to the use of isotopes of these elements in therapeutic and diagnostic nuclear medicine.", Nucl. Med. Biol. 13(4), 1986, 465-477.

10. Wolf, W., Shani, J., "Criteria for the selection of the most desirable radionuclide for radiolabeling monoclonal antibodies.", Nucl. Med. Biol. 13(4),1986,319-324.

11. Troutner, D.E., "Chemical and physical properties of radionuclides.", Nucl. Med. Biol. 14(3), 1987, 171-176.

12. Adelstein, S.J., Kassis, A.I., "Radiobiologic implications of the microscopic distribution of energy from radionuclides.", Nucl. Med. Biol., 14,(3),1987,165-69.

13. Neumann, R.D., Gottschalk, A., Diagnostic techniques in nuclear medicine., Ann. Rev. Nucl. Part. Sci., 1979, 29, 283-312.

14. Cotton, F.A., Wilkingson,G., Advanced Inorganic Chemistry: A Comprehensive Text., 4th Ed., Wiley, New York, 1980.

15. Colton, R., The Chemistry of Rhenium and Technetium., Interscience Publishers, 1965.

16. Vanderheyden, J.L., Heeg, M.J., Deutsch, E., "Comparison of the chemical and biological properties of *trans*-$[Tc(DMPE)_2Cl_2]^+$ and *trans*-$[Re(DMPE)_2Cl_2]^+$, where DMPE = 1,2-bis(dimethylphosphine)ethane. Single crystal structural analysis of *trans*-$[Re(DMPE)_2Cl_2]PF_6$.", Inorg. Chem. 24,1985,1666-1673.

17. Eisenhut, M., "Preparation of ^{186}Re-perrhenate for nuclear medical purposes.", Int. J. Appl. Rad. Iso., 33,1982,99-103.

18. Harvey, B.G., Introduction to Nuclear Physics and Chemistry., 2nd Ed., Prentice-Hall Inc., New Jersey, 1969.

19. Wessels. B.W., Rogus, R.D., "Radionuclide selection and model absorbed dose calculations for radiolabeled tumor associated antibodies.", Med. Phys. 11(5), 1985, 638-645.

20. Graham, P., Abeysekera, B., Porter, J.K., NORDION International Inc. TRIUMF, Private Communication (via Tom Ruth, TRIUMF, Vancouver, B.C.).

21. Ruth, T.J., Private Communication

22. Friedlander G., Kennedy, J.W., Macias, E.S., Miller, J.M., Nuclear and Radiochemistry, 3rd ed., John Wiley and Sons, 1981.

23. Ravn, H.L., "Experiments with intense secondary beams of radioactive ions.", Physics Reports, 54, (1979), 201-259.

24. Weast, R.C. ed., CRC Handbook of Chemistry and Physics, 67th Ed., CRC Press, Boca Raton, Florida, 1986.

25. Silberberg, R., Tsao, C.H., "Partial cross-sections in high energy nuclear reactions and astrophysical applications. I. Targets with $Z \leq 28$.", Astrophys. J. Suppl. 25, 1973, 315-333.

26. Silberberg, R., Tsao, C.H., "Partial cross-sections in high energy nuclear reactions and astrophysical applications. II. Targets heavier than Ni.", Astrophys. J. Suppl. 25, 1973, 335-368.

27. Reus, U., Westmeier, W., "Catalog of gamma rays from radioactive decay., Atomic Data and Nuclear Data Tables, 29, (1983), pp 13ff.

28. Kaufman, S.B., Steinberg, E.P., "Cross-section measurements of nuclides formed by the reaction of 0.20 - 6.0 GeV protons with ^{197}Au.", Phys. Rev., C22, (1980), 167-78.

29. Asano, Yuzo, et. al., "Spallation and fission yields in the interactions of tantulum, tungsten, and gold with 500 MeV protons.", J. Phys. Soc. Jap., 54(10), 1985, 3734-3741.

30. Miller, D.A., et. al., "Nuclear spallation as a mechanism for radioisotope production: cross-sections for selected nuclides.", J. Radioanal. Nuc. Chem. 123, (1978), 643-653.

31. Ruth, T.J., Private Communication

32. Kusaka, Y., Meinke, W.W., Rapid Radiochemical Separations, NAS-NS 3104, 1961.

33. The Radiochemical Manual Part 2: Radioactive Chemicals., The Radiochemical Centre, Amersham, Buckinghamshire, 1963.

34. Bayar, B., Novgorodov, A.F., Zaitseva, N.G., "Rapid gas-thermochromatographic separation of radioactive elements. I. production of radioactive Re isotopes.", Radiochem, Radioanal. Letters, 15(1973), 231-42.

35. Bayar, B., Novgorodov, A.F., Vocilka, I., Zaitseva, N.G., "Rapid gas-thermochromatographic separation of radioactive elements. II. Gold as a universal target for the rapid producing of Re, Os, Ir, and Hg isotopes.", Radiochem. Radioanal. Letters, 19(1),1974, 43-53.

36. Bayar, B., Votsilka, I., Zaitseva, N.G., Novgorodov, A.F., "Rapid gas thermochromatographic methods of isolating radioactive elements. V. Formation of volatile oxides and hydroxides of rhenium in the system rhenium-tungsten and their gas thermochromatographic behavior.", Soviet Radiochem., 16,1975,871-876.

37. Novgorodov, A.F., Adilbish, *., Zaitseva, N.G., Kowalew, A., Kovacs, Z., "Investigation of the behavior of nuclear reaction products at their volatilization from irradiated Ag and Au targets in dynamic vacuum (10^{-2}-10^{-3} torr O_2 or H_2O).", J. Radioanal. Chem., 56,1980,37-51.

38. Steffen, A., Bächmann, K., "Gas chromatographic study of volatile oxides and hydroxides of Tc, Re,Ru, Os, and Ir. I. Investigation by isothermal gas chromatography.", Talanta, 25(1978),551-556.

39. Steffen, A., Bächmann, K., "Gas chromatographic study of volatile oxides and hydroxides of Re, Tc, Os, Ru, and Ir. II. Thermochromatographic investigation.", Talanta, 25,1978,677-683.

40. Chart of the Nuclides, 12th Ed., General Electric Co., San Jose, California, 1977.

41. Perovic, B., "The scientific and technical foundations of electromagnetic isotope separation technolgy.", Vacuum, 33, (1983), 511-519.

42. Cumming, J.B., "Monitor reactions for high energy proton beams", Annual Review of Nucl. Science., 13, (1963), 261-286.

43. Cackette, Mike, Development of an Analytical Method for the Analysis of Gold. M.Sc. Thesis (in preparation), Department of Chemistry, S.F.U., 1989.

44. Gunnink, R., Niday, J.B., UCRL Report no. 51061, 1972 (unpublished).

45. Cumming, J.B., "CLSQ the brookhaven decay curve analysis program", Applications of Computers to Nuclear And Radiochemistry NAS-NS 3107 (1962), 25-33.

46. Rogers, Paul C., "Frantic program for analysis of exponential growth and decay curves", M.I.T. Tech Report 76 (NYO-2303), 1962.

47. Bertin, Eugene P., Introduction to X-Ray Spectrometric Analysis., Plenum Press, New York, 1978, pp 316-317.

48. Schell, C., The Formation of Rhenium Oxides. B.Appl.Sc. Thesis, Department of Chemical Engineering, U.B.C., 1988, (unpublished).

49. Baird, D.C., Experimentation, an Introduction to Measurement Theory and Experiment Design., Prentice-Hall, 1962.

50. Janni, Joseph F., "Proton range-energy tables 1 keV - 10 GeV. Part 2 for elements $1 \leq Z \leq 92$.", Nuc. Data Tables, 27, 341-529, (1982).

51. Oxorn, K., Crawford, J.E., Dautet, H., Lee, J.K.P., Moore, R.B., Nikkinen, L., Buchman, L., D'Auria J.M., Kokke, R., Otter, A.J., Sprenger, H., Vincent, J., "The installation of a prototype on-line separator at TRIUMF (TISOL).", N.I.M., B26,1987,143-50.